iberiancomsolconference.es

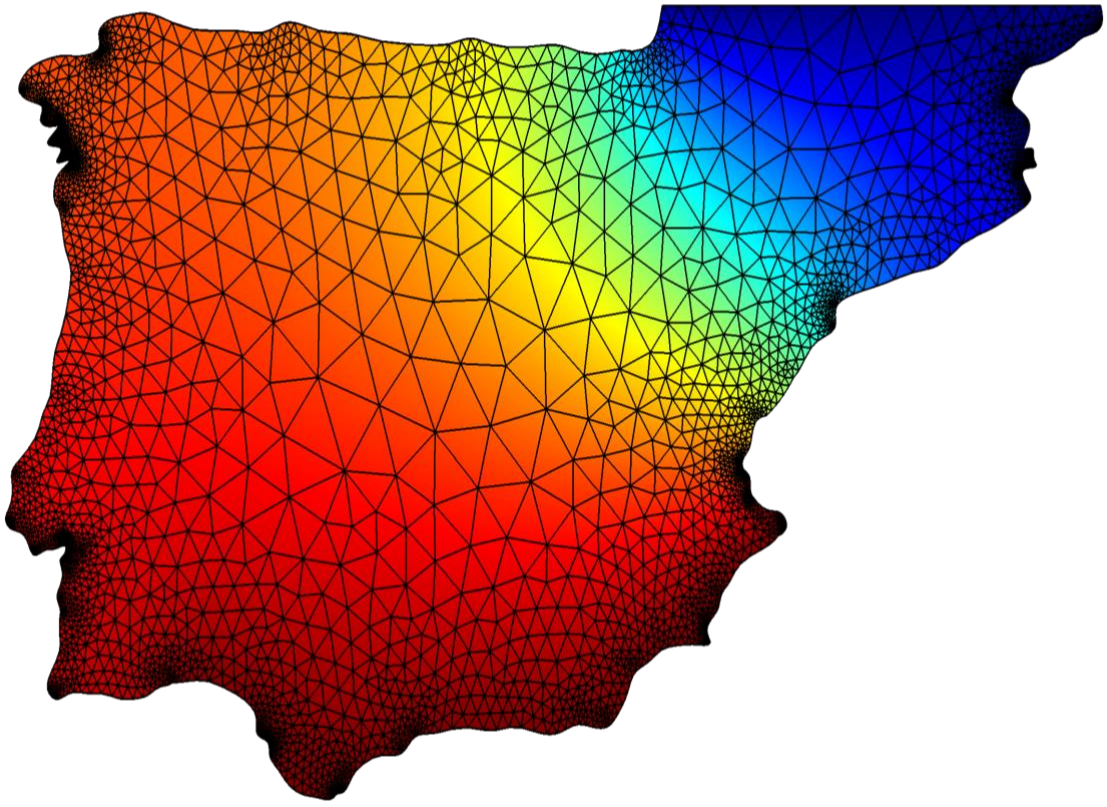

Iberian COMSOL Multiphysics CONFERENCE

Málaga. June 28, 2024

UNIVERSIDAD DE MÁLAGA

Multiphysics Modeling School

ESCUELA DE INGENIERÍAS INDUSTRIALES

INSTITUTO CARLOS I DE FÍSICA TEÓRICA Y COMPUTACIONAL

Iberian
COMSOL Multiphysics
CONFERENCE
Málaga. June 28, 2024

Iberian COMSOL Multiphysics Conference 2024

Málaga. June 28, 2024

Conference Proceedings

Proceedings of the Iberian COMSOL Multiphysics Conference 2024
Addlink Software Científico
Maria Aurèlia Capmany, 2-4, local, Barcelona, 08001, Barcelona
ISBN 978-84-09-64038-6

Iberian
COMSOL Multiphysics
CONFERENCE
Málaga. June 28, 2024

Table of Contents

Iberian
COMSOL Multiphysics
CONFERENCE
Málaga. June 28, 2024

Welcome to the Iberian COMSOL Multiphysics Conference 2024 in Málaga!

It is a great pleasure to welcome you to the leading event in Southern Europe on Multiphysics Modeling and Simulation in Science and Engineering: the Iberian COMSOL Multiphysics Conference 2024. It was held on June 28 at the Rectorate of the University of Malaga, Malaga, Spain. The conference is co-organized by the University of Málaga and the companies Addlink Scientific Software (Barcelona, Spain) and COMSOL AB (Stockholm, Sweden).

The Iberian COMSOL Multiphysics Conference offers a unique space for professionals interested in multiphysics modeling, where they can learn about the latest technology for multiphysics simulation, share personal experiences in the field of finite element simulation and foster a climate of networking. The Iberian COMSOL Multiphysics Conference is a meeting forum for the community of COMSOL Multiphysics users from both academia and industry.

Our goal has been to bring together a broad and scientifically diverse community in an event that promotes the exchange of inspiring experiences in the use of COMSOL Multiphysics. To this end, we have been delighted to hold this world-class international event once again for multiphysics modelling and simulation. It has been a great forum to connect with COMSOL Multiphysics users and to participate in training opportunities and activities designed specifically for the professional engineering and scientific-academic community. Oral and poster presentations exemplified novel achievements in multiphysics modelling and simulation with COMSOL Multiphysics.

In addition to being inspired by new methods, ideas and knowledge, attendees were able to discover and enjoy the city of Málaga. Its origins date back to the Phoenician and Punic sites from the time of the founding of the city. Later it was a Roman municipality with great commercial activity and during the Arab period it became the capital of a small independent kingdom. Since the 1960s, it has been an international tourist destination and the centre of one of the most prosperous regions of southern Spain. Málaga is a city for all tastes, with activities for everyone, and a perfect city for shopping while exploring the historic centre. Málaga has become a city of museums with more than twenty of them. Only in the historic centre, there are up to 24 museums that make Málaga one of the most developed cities in its museum offer: Picasso Museum, Carmen Thyssen Museum, Pompidou Centre, Contemporary Art Centre, Automobile and Fashion Museum, etc.

Finally, we would like to express our thanks to Addlink Scientific Software, COMSOL AB, the Technical Secretariat of El Corte Inglés, the University of Málaga and its School of Industrial Engineering, the Multiphysics Modeling School, the Institute Carlos I for Theoretical and Computational Physics (iC1), the Organizing and Scientific Committees and all the speakers for their contribution and assistance. Also, to all the helping hands, whose efforts have undoubtedly made the Iberian COMSOL Multiphysics Conference 2024 a conference to remember.

The Organizing Committee of the Iberian COMSOL Multiphysics Conference 2024.

Iberian
COMSOL Multiphysics
CONFERENCE
Málaga. June 28, 2024

Conference Program

Friday morning, June 28, 2024	
9:00	**Registration opens**
9:15 – 9:30	**Welcome and opening remarks**
9:30 – 10:30	**Minicourse 1** Parameter estimation for nonlinear phenomena Ed González, COMSOL
10:30 – 11:30	**Oral presentations 1**
11:30 – 12:30	**Poster session** (with coffee break)
12:30 – 13:30	**Plenary Session** Modeling Hydrogen Embrittlement with COMSOL Multiphysics Emilio Martínez-Pañeda, University of Oxford
13:30 – 14:30	**Oral presentations 2**
14:30 – 16:00	**Lunch**

Friday afternoon, June 28, 2024	
16:00 – 16:45	**Oral presentations 3**
16:45 – 17:45	**Minicourse 2** Surrogate models to accelerate model and app computations Alejandro Cifuentes López, Addlink Software Científico
17:45 – 18:00	**Surrogate Modeling Case Study** Solar Cell Performance Analysis Pablo Ferrada, Addlink Software Científico
18:00– 18:30	**Oral presentations 4**
18:30	**Closing remarks**
21:00	**Gala dinner**

Plenary Session and Minicourses

Minicourse 1: Parameter estimation for nonlinear phenomena

Dr. Ed González

Mechanical systems often contain components that exhibit nonlinear material behavior. Examples include large elastic deformations in seals and gaskets, strain-rate dependence and hysteresis during cyclic loading in rubbers and soft biological tissues, and elastoplastic flow and creep in metals.

Most of these constitutive relations stem from a phenomenological approach, focusing on fitting mathematical equations to experimental data to describe the macroscopic nature of the material. Therefore, it is essential to calibrate and validate the chosen material model against experimental data to predict the behavior of such components in complex finite element models.

The latest version of the COMSOL Multiphysics software features significantly enhanced parameter estimation capabilities. Improvements to the optimization solvers can greatly boost the performance of parameter estimation from experimental data, encompassing uniaxial, biaxial, and cyclic load cases.

The minicourse will comprehensively explore the general theory and intricacies of parameter estimation functionalities, offering live demonstrations for practical application.

Dr. Ed González

Director of Development, Structural Mechanics, at COMSOL AB, Stockholm (Sweden)

PhD in Physics from the Ludwig-Maximilians-Universität of Munich, Germany. He is currently the Director of Development for the Structural Mechanics products.

He regularly presents the numerical capabilities of COMSOL Multiphysics at multiple conferences, courses, and webinars.

During his extensive tenure at COMSOL AB, Sweden, where he served as both Product Manager and Technology Manager, he successfully led a multitude of projects across diverse disciplines. These included acoustics, fluid dynamics, electromagnetism, structural mechanics, mass transport, and heat transfer.

He is also member of the teaching staff of the Multiphysics Modeling School, University of Málaga.

Plenary Session: Modeling Hydrogen Embrittlement with COMSOL Multiphysics

Prof. Emilio Martínez-Pañeda

Hydrogen is deemed to play a key role in decarbonization strategies due to its abundance, eco-friendliness, diverse production sources, and multifaceted applications. However, it is also infamous for "embrittling" metallic materials, dramatically reducing their ductility, fracture toughness and fatigue crack growth resistance.

This talk will show how computational tools, and particularly COMSOL Multiphysics, can be used to predict hydrogen-material interactions rigorously and accurately; resolving the underlying physics of hydrogen absorption, diffusion, and the resulting embrittlement. Model predictions will be compared with a wide range of experiments on samples exposed to hydrogen-containing environments, showcasing the success of multi-physics phase field-based approaches in enabling predictive modelling.

Large-scale case studies of engineering interest will also be addressed to demonstrate the potential of these models in enabling Virtual Testing in hydrogen-containing environments, enabling the safe and accelerated deployment of hydrogen energy infrastructure, a pressing societal need.

Prof. Emilio Martínez-Pañeda

University of Oxford (UK)

Prof Emilio Martinez-Pañeda is an Associate Professor at the University of Oxford. Prior to joining Oxford, he was a Reader (Associate Professor) at Imperial College London, where he led an interdisciplinary research group from 2019 to 2023 (2019: Lecturer, 2021: Senior Lecturer, 2023: Reader). Before that, he was an 1851 Research Fellow at the University of Cambridge.

Prof Emilio Martinez-Pañeda's research spans a wide range of challenges lying at the interface between mechanics and other disciplines such as biology, geology, chemistry and materials science, being particularly known for his pioneering contributions to the area of hydrogen embrittlement.

Prof Emilio Martinez-Pañeda has been the PI on over 4.5M GBP of funding in the past five years (ERC Starting Grant, UKRI) and his work has been recognized through multiple awards, including the 2021 UK Young Engineer of the Year (Royal Academy of Engineering), the 2022 Imperial College President's Medal for Excellence in Research (Early Career), the 2021 Gustavo Colonnetti Medal (RILEM), the 2020 IMechE Prestige Award, the 2020 Simo Prize (SEMNI), and the 2023 Young Investigator Medal by Spain's Royal Academy of Engineering. In 2021, he was elected a Fellow of the Institute of Materials, Minerals and Mining (FIMMM).

Minicourse 2: Surrogate models to accelerate model and app computations

Dr. Alejandro Cifuentes López

COMSOL Multiphysics version 6.2 introduces powerful new functionality for creating and using surrogate models. This functionality is available through solvers based on design of experiments (DOE) as well as function definitions. The computational speed of an app can be greatly increased by using a surrogate model instead of a full-fledged finite element model. A surrogate model is a simpler, usually computationally less expensive model that is used to approximate the behavior of a more complex, and often more computationally expensive, model. The faster model evaluation offered by a surrogate model provides the app user with a more interactive experience and makes it easier to spread the use of simulation throughout an organization.

A surrogate model is created by training on a large dataset produced using the *Surrogate Model Training* study.

The use of surrogate model functions is not limited to apps and uncertainty quantification but can also be used to represent material data, for optimization, and more. Note that the surrogate model functions can be differentiated multiple times with respect to any of the input parameters.

The minicourse will include the fundamental theory and description of the generation and use of surrogate models, as well as some live examples.

Dr. Alejandro Cifuentes López

Technical Engineer at Addlink Software Científico, Barcelona (Spain)

PhD in Chemical Process Engineering from the Polytechnic University of Catalonia, and Master's Degree in Renewable Energies and Energy Sustainability from the University of Barcelona. He has been an associate professor at the Polytechnic University of Catalonia, teaching the course on Computational Simulation in Fluid Mechanics and Heat Transfer. At Addlink Software Científico, he has conducted numerous seminars and courses on various aspects of the COMSOL Multiphysics simulation platform. The training content included a general introduction to the main platform, the use of CFD, heat transfer and chemical engineering modules, as well as the application builder.

He specializes in the simulation of reactive transport of chemical species with surface reactions or in porous media, such as in the case of a fluidized bed reactor. These are complex models as there is a strong coupling between different physics, making convergence challenging. Additionally, he has conducted numerous optimization studies and parameter tuning in various areas.

He is also member of the teaching staff of the Multiphysics Modeling School, University of Málaga.

Abstracts

Oral presentations

O1: *Multiphysics Modeling of a Novel Non-Aqueous Redox Flow Battery (NAQRFB)*, Mirko D'Adamo, Nicolas Daub, Juan M. Paz-García, Lluís Trilla, José Sáez.

O2: *Electrodialysis with Bipolar Membranes for Skim Milk Acidification: A 2-D Computational Model,* Tamara León, Ricardo Torres, Arthur Merkel, Lluís Jofre, José Luis Cortina, Lukáš Dvořák, Lilia Ahrné.

O3: *Modelling and Numerical simulation of a toluene direct electro-hydrogenation Electrolyzer cell,* Antonio Atienza-Márquez, Takuto Araki.

O4: *2D Simulation of Tertiary Current Distribution on a Three-compartment Electrolyzer for CO_2 Electroreduction to Formic Acid*, Camilo Peralta, Esther Santos, Ángel Irabien.

O5: *Modeling of Electrodialytic Desalination of Wastewater Effluent,* Elena Olivares-Ligero, María Villén-Guzmán, María J. Martínez-Salverri, Juan A. Baez Durán, José M. Rodríguez-Maroto, María M. Cerrillo-González, Juan M. Paz-García.

O6: *A Simulation of the Spatial Distribution of Chemical Species During the Corrosion of the Zn-Fe Galvanic Couple,* Alexandre Bastos, Juan M. Paz-García, Emilio Ruiz-Reina.

O7: *An Effective Simulation Framework for Fluid Flow in Microwave-Heated Packed Beds,* Carlos González-Niño.

O8: *Modelling and Simulation of a Packed Bed Adsorption column for edible oil decolorization,* Carlos Macías.

O9: *Multiphysics Modeling of Microwave Technology for Sustainable Revalorization of Metal Casting Molding Sands,* P. Garcia-Michelena, I. Crespo, G. Arruebarrena, I. Vicario, X. Chamorro, I. Hurtado.

O10: *Nonlinear Dependence of Flow Velocity in Electrothermoplasmonics with Gold Nanoparticles Suspension*, Carlos D. González-Gómez, Raúl A. Rica, Emilio Ruiz-Reina.

O11: *Modeling of an Acoustic Leaky-Wave Antenna for Spatial Localization*, Alejandro Fernández-Garrido, María Campo-Valera, Elena Abdo-Sánchez, Rubén Picó, Rafael Asorey-Cacheda.

Surrogate Modeling Case Study O12: *Surrogate Modeling Applied to Solar Cell Performance Analysis Using COMSOL Multiphysics,* Pablo Ferrada, Alejandro Cifuentes, Benjamin Ivorra.

O13: *Acoustic Metamolecule Made of Eight Nanopillars Mediated by Surface Waves: High-Quality Resonances,* Ricardo M. Abraham-Ekeroth, Liangshu He, Dani Torrent.

O14: *Elastocaloric Effect at the Nanoscale in Cu–Al–Ni Shape Memory Alloys Modeled with COMSOL Multiphysics*, Jose F. Gómez Cortés, Emilio Ruiz-Reina, Eduardo González, María L. Nó, Jose M. San-Juan.

Poster presentations

P1: *Modelling and Simulation of a Fixed Bed Photocatalytic reactor: Influence of Some Design Variables on its Performance*, Carlos Macías, Alejandro Cifuentes-López.

P2: *Exploring Heterogeneous Graphite Electrodes: Parametric Sweeping and Stochastic Generation Techniques for Simulation and Analysis Using COMSOL*, Álvaro Abucide-Armas, Oier Arcelus, Ander Sánchez-Chica, Javier Carrasco, Ekaitz Zulueta.

P3: *Optimization of Energy Transmission through Waveguides, Antennas, and Dielectric Materials: An Integrated Approach to Wave Miniaturization*, Alberto Frisa-Rubio, Carlos González-Niño.

P4: *Dry Reforming of Biogas over Structured Catalysts: CFD Modelling and Simulation of Channels with Extreme Thermal Conditions*, Felipe Costa, Andrea Navarro-Puyuelo, Inés Reyero, Fernando Bimbela, Luis M. Gandía.

P5: *Numerical Simulation and Experimental Validation of a Micromachining Process on PDMS Membranes by Femtosecond Pulse Laser Ablation*, Daniel Sánchez, Chahinez Berrah, Javier Rodríguez, Andrés Sanz-García.

P6: *Laser Spot Step Heating Thermography for Visualizing Heat Convection in a Fluid*, A. Bedoya, J.B. Rojas-Trigos, J. Hernández-Wong, A. Calderón, E. Marín.

P7: *Computational-Aided Design of Continuous-Flow Systems for the Magnetic Recovery of Microplastics from Water*, Cristina González-Fernández, Eugenio Bringas, María J. Rivero, Inmaculada Ortiz.

P8: *Application of COMSOL Multiphysics in Electrical Infrastructure Simulation for Newly Graduated Engineers*, Safaa El Ouariachi.

P9: *Design and Proof of Concept of Micro-Dampers based on Nano-Pillars of Shape Memory Alloys to Improve MEMS Reliability*, Jose M. San-Juan, Jose F. Gómez-Cortés, Emilio Ruiz-Reina, Eduardo González y Maria L. Nó.

P10: *Using COMSOL Multiphysics to Simulate the Superelastic Behavior in Shape Memory Alloys for Aerospace Applications*, Ander Abadín, José F. Gómez-Cortés, María L. Nó, José M. San-Juan.

P11: *Analyzing Total Hip Arthroplasty: Straight Stem vs Anatomical Stem with Different Materials and Activities*, Pedro Queirós, Nuno Gueiral, Carlos David González-Gómez.

P12: *THCM Modelling of Nuclear High-Level Waste cells*, Miquel de la Iglesia, Marcelo Laviña, Joan Pelegrí, Emilie Coene, Arnau Pont, Andrés Idiart, Benoit Cochepin.

P13: *Optimal Resistive Load for Maximizing the Power Output of a Piezoelectric Harvester*, Claudia Săvescu, Daniel Comeagă, Mihaela Roman, Adrian Săvescu.

P14: *Thermoelectric Generator Simulations with and without Heatsink*, Mihaela Roman, Claudia Săvescu, Adrian Săvescu, Remus Stoica, Daniel Comeagă.

Multiphysics Modeling of a Novel Non-Aqueous Redox Flow Battery (NAQRFB)

Mirko D'Adamo[1,2 *], Nicolas Daub[3], Juan Manuel Paz[4], Lluís Trilla[2], Jose Saez[1]

[1]Smart Energy, N Vision Systems And Technologies, Barcelona, Spain,
[2]IREC - Fundació Institut de Recerca en Energía de Catalunya, Sant Adrià del Besòs, Spain
[3]Molecular Materials and Nanosystems & Institute for Complex Molecular Systems, University of Technology, Eindhoven, The Netherlands
[4]Department of Chemical Engineering, Universidad de Malaga, Malaga, Spain
[*]Corresponding author: mirko.dadamo@nvision.es

Introduction

The Non-Aqueous Redox Flow battery (NAQRFB) is a significant advancement over conventional systems due to its ability to operate within a larger voltage window. This study focuses on the combination of N-(2-(2-methoxyethoxy) ethyl)phenothiazine(MEEPT) with a terephthalonitrile derivative, which has yielded a battery cell [1] with a 2.4 V potential (Figure 1), demonstrating remarkable efficiency and cycle life.

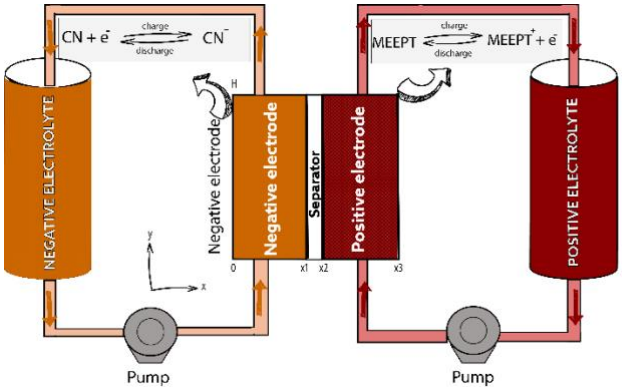

Figure 1: NAQRFB cell.

Use of COMSOL Multiphysics

A 2D-Multiphysics model was developed in COMSOL Multiphysics to enhance our understanding of the battery's internal workings and pave the way for future scalability. In particular, this study shows the crossover of different species across the cell [2]. The model incorporates the Nernst-Planck equation, which accounts for diffusion, convection, and migration of ions. It also includes the charge conservation equation in the bulk electrolyte and in the porous electrode, the electroneutrality condition, and the current density in the electrolyte and porous electrode given by the Faraday's Law and the Ohm's Law, respectively.

Results

After setting the initial real parameters, the model was optimized by adjusting parameters such as the exchange current density and charge transfer for both positive and negative electrodes, using data from one complete cycle. The final model has a Root Mean Square Error (RMSE) Voltage

of 2%. Figure 2 shows the distributions of MEEPT in the left column and CN in the right column at different states of charge (SoC). It is interesting to observe the crossover of various species from one electrode to the other, resulting in capacity fade [3].

Conclusion

This study highlights the intriguing phenomenon of crossover in the NAQRFB, which leads to capacity fade. The 2D Multiphysics model used to simulate the NAQRFB provides a comprehensive understanding of its operation. The model has been validated against real data with a 2% RMSE voltage, demonstrating its accuracy and reliability. This model will be instrumental in optimizing the cell design, taking into account factors such as optimal current density and flow rate, thereby enhancing both design and performance. This work lays the groundwork for future cell scale-up.

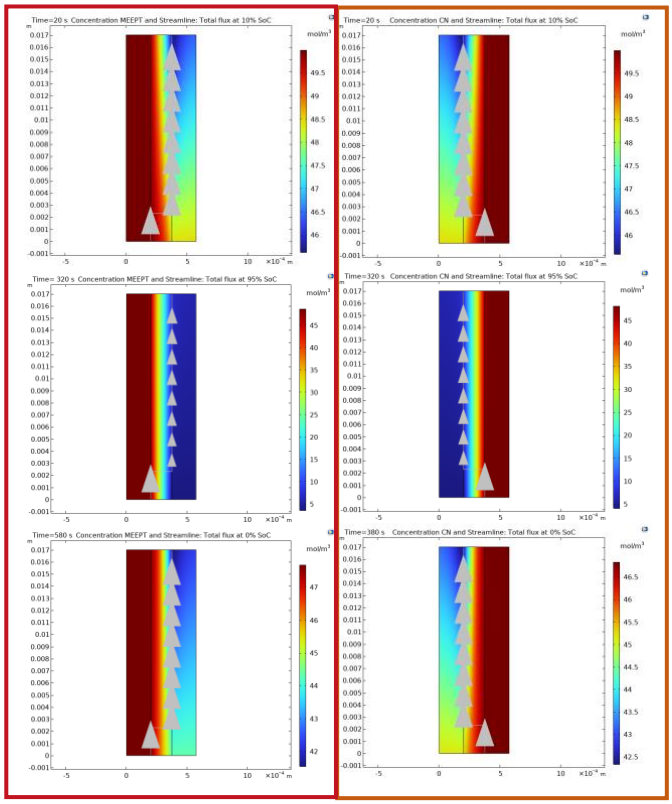

Figure 2: MEEPT and CN concentrations at 0% , 95% and 0% SoC

References

1. J. D. Milshtein et al., “High current density, long duration cycling of soluble organic active species for non-aqueous redox flow batteries,” Energy & Environmental Science, **9**(11), pp. 3531–3543, Jan. 2016.
2. Knehr, K. W. and Kumbur, Open circuit voltage of vanadium redox flow batteries: Discrepancy between models and experiments, E. C., Electrochemistry Communications, **13** (2011) 342
3. Modak, S.V., Shen, W., Singh, S. et al. Understanding capacity fade in organic redox-flow batteries by combining spectroscopy with statistical inference techniques. Nat Commun 14, 3602 (2023).

Electrodialysis with Bipolar Membranes for Skim Milk Acidification: A 2-D Computational Model

Tamara León[1*], Ricardo Torres[2], Arthur Merkel[3], Lluís Jofre[2], José Luis Cortina[1], Lukáš Dvořák[4], Lilia Ahrné[3]

[1]Chemical Engineering Department, Escola d'Enginyeria de Barcelona Est (EEBE), Universitat Politècnica de Catalunya (UPC)-BarcelonaTECH,
[2]Department of Fluid Mechanics, Escola d'Enginyeria de Barcelona Est (EEBE), Universitat Politecnica de Catalunya (UPC)-BarcelonaTech,
[3]Department of Food Science, University of Copenhagen,
[4]Institute for Nanomaterials, Advanced Technologies and Innovation, Technical University of Liberec.
*Corresponding author: tamara.elizabeth.leon@upc.edu

Introduction

Electrodialysis has become a relevant technology in promoting sustainability within the food industry [1]. Bipolar membrane electrodialysis offers an efficient and eco-friendly alternative for skim milk acidification, eliminating the need for added acids that affect milk composition and properties [2]. For the first time, this study presents a comprehensive 2-D computational model to investigate the multi-ionic transport and dynamics of skim milk electro-acidification using bipolar membrane electrodialysis.

Use of COMSOL Multiphysics

The model is based on conservation equations for mass-charge transport, coupled with the description of water splitting through the second Wien effect. Simulations were carried out at the 6.0 version of COMSOL Multiphysics. The Tertiary Current Distribution was the Physics selected for the model, and special emphasis was placed on the mesh refinement at the bulk-membrane interface.

Conclusions

The primary focus of the analysis was on the skim milk pH evolution and the concentration profiles of the major ions. The results showed that ion concentration values varied due to concentration polarization and differences in ion mobilities. The simulations were compared with experimental data, showing reasonable agreement, particularly for Ca^{2+} ion concentration. Despite excluding organic components in its analysis, this model offers a novel and valuable approach to the study of skim milk electro-acidification using bipolar membrane electrodialysis, providing essential insights for process understanding and optimization.

References

1. Bazinet L, Lamarche F, Ippersiel D. Bipolar-membrane electrodialysis: Applications of electrodialysis in the food industry. Trends Food Sci Technol. 1998; **9**(3):107–13.

2. Bazinet L, Ippersiel D, Gendron C, René-Paradis J, Tétrault C, Beaudry J, et al. Bipolar membrane electroacidification of demineralized skim milk. J Agric Food Chem. 2001; **49**(6):2812–8.

Modelling and numerical simulation of a toluene direct electro-hydrogenation electrolyzer cell

Antonio Atienza-Márquez[1*] and Takuto Araki[2]

[1]Universidad de Málaga, GEUMA, C/ Doctor Ortiz Ramos s/n, Málaga, 29071, Spain.
[2]Yokohama National University, Faculty of Engineering, Yokohama, 240-8501, Japan.
*Corresponding author: atienza-marquez@uma.es

Introduction

Hydrogen technologies will play a pivotal role in the transition towards a decarbonized economy. However, the volumetric energy density of hydrogen is extremely low, which complicates its storage and transport. Regarding the bulk and long-distance transport of hydrogen, the organic hydride toluene/methylcyclohexane (MCH) is one the most promising liquid organic hydrogen carriers (LOHCs) because of its low-toxicity, acceptable hydrogen storage capacity and its gasoline-like features that will allow using the existing oil infrastructure.

Figure 1 shows a schematic diagram of a direct toluene electro-hydrogenation electrolyzer based on proton exchange membrane technology [1]. Concerning the conventional two-step toluene hydrogenation technique (i.e., hydrogen production via electrolysis and subsequent exothermic toluene hydrogenation), this innovative single-step method offers advantages in terms of a lower theoretical decomposition voltage and avoids heat losses [2]. Yet, in practice, sufficient toluene supply to the cathode reaction site (i.e., the catalyst layer) is crucial regarding the hydrogenation ratio. This work presents the modeling and preliminary numerical simulation outcomes of a direct toluene electro-hydrogenation electrolyzer cell.

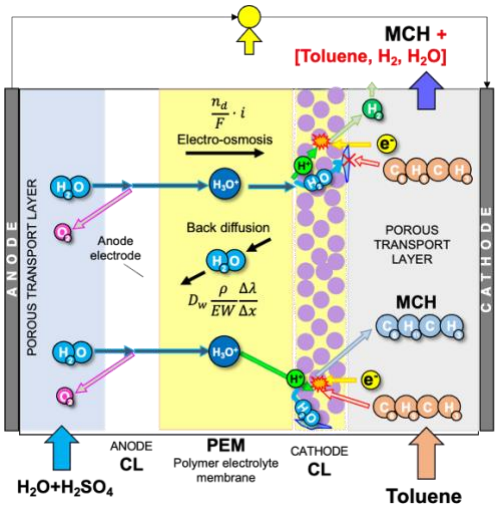

Figure 1: Schematic diagram of a direct toluene electro-hydrogenation electrolyzer.

Use of COMSOL Multiphysics

A 2-dimensional model of a single direct toluene electro-hydrogenation electrolyzer cell was developed in COMSOL Multiphysics (Fig. 1(a)). The model couples the different mechanisms and equations that describe the behavior of the system: continuity equations for the water and oil

phase, the convection-diffusion equation to determine the concentration of toluene and MCH in the cathode side (both the CL and the PTL), the water transport across the polymeric electrolyte membrane, and the electric current conservation equations. The numerical simulation outcomes will report the concentration of species in the cathode side (i.e., oil-phase and liquid water accumulation), water uptake in the membrane, and current density distribution in the cathode electrode.

Results

Figure 2 depicts the concentration of toluene and MCH obtained at the cathode side from the inlet (bottom) to the outlet (top) when the cell operates under a current density of 0.5 A/cm². While the concentration of toluene decreases as the stream approaches the outlet, the concentration of MCH increases. Indeed, the MCH concentration is maximum at the cathode's outlet. On the other hand, the concentration of toluene is higher in those regions closest to the cathode flow field plate, while the highest concentration of MCH was found near the catalyst layer.

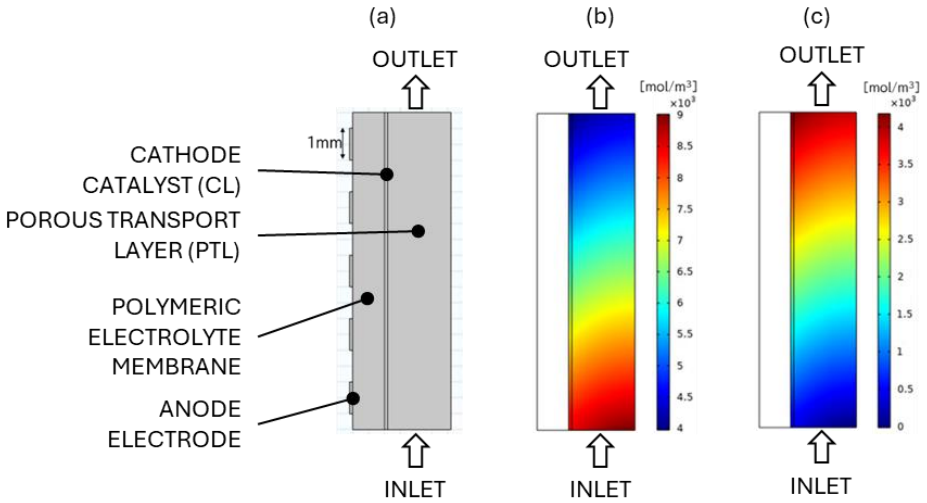

Figure 2: (a) Two-dimensional geometry of the direct toluene electro-hydrogenation cell modelled. Concentration of the oil-phase at the cathode side under 0.5 A/cm^2: (b) toluene and (c) MCH

Conclusion

In combination with experimental data, the numerical simulations of a direct toluene electro-hydrogenation electrolyzer cell provide helpful information to understand the performance and plan strategies to optimize the design of that technology. The future versions of the modeling will include the gas phase (i.e., hydrogen bubbles) at the cathode side, which inhibits the toluene mass transfer towards the reaction sites.

References

1. F. Reyna-Peña, A. Atienza-Márquez et al., In situ X-ray CT visualization of hydrogen bubbles inside the porous transport layer of a direct toluene electro-hydrogenation electrolyzer, *International Journal of Hydrogen Energy*, **50**, 787-798 (2024).

2. K. Shigemasa, A. Atienza-Márquez et al., Visualization of dragged water and generated hydrogen bubbles in a direct toluene electro-hydrogenation electrolyzer, *Journal of Power Sources*, **554**, 232304 (2023).

2D Simulation of Tertiary Current Distribution on a three-compartment Electrolyzer for CO_2 Electroreduction to Formic Acid

Camilo Peralta[1,2], Esther Santos[1,2], Ángel Irabien[1]

[1]Departamento de Ingenierías Química y Biomolecular, Universidad de Cantabria, ETSIIyT, Avenida de Los Castros s/n, Santander 39005, Spain
[2]APRIA Systems SL, Parque Empresarial de Morero P2-13, Nave 3-8, 39611, Astillero, Cantabria, Spain

Introduction

CO_2 electrolyzers offer numerous advantages by directly converting CO_2 into various value-added products using renewable energy [1]. In this process, several products such as carbon monoxide, formic acid, methanol, ethanol, etc., can be produced through multiple electron-transport steps. The CO_2 reduction process usually employs liquid electrolytes such as potassium bicarbonate or potassium hydroxide. However, the liquid products formed during CO_2RR can mix with the aqueous electrolyte, requiring downstream separation processes that increase the cost of the CO_2RR [2]. To address this issue, solid-state electrolyzer (SSE) has been recently employed [3,4]. In this configuration, formate ions generated at the cathode are transported through an Anion Exchange Membrane (AEM) to a central compartment. Meanwhile, protons (H^+) produced in the anode compartment are transported through a Proton Exchange Membrane (PEM) and react with formate ions in the central compartment to produce pure formic acid (Figure 2).

Use of COMSOL Multiphysics

In this study, it has been used COMSOL Multiphysics® to evaluate the formate concentration within the central compartment, varying the applied potential and the concentration of fixed charges in the membrane.

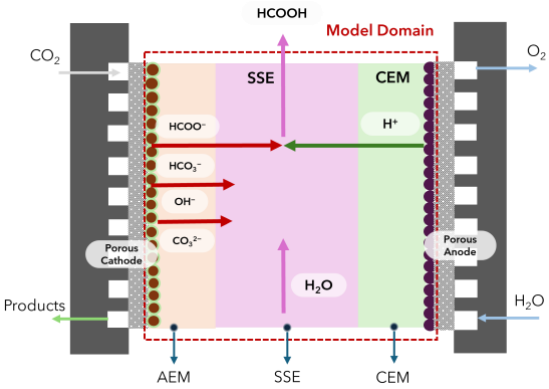

Figure 2: Model domain.

The electrochemical reduction of CO_2 to formate in a three-compartment electrolyzer has been simulated. A stationary current distribution initialization study was performed using COMSOL Multiphysics®. The entire domain was modeled using Tertiary Current Distribution, Nernst-Planck interface. The concentration-dependent Butler-Volmer equation was used for both CO_2 reduction to formate and the hydrogen evolution reaction (HER). The homogeneous buffer reaction producing (bi)carbonate was included employing the law of mass action. The Donnan

boundary condition at the membrane domain boundaries was applied. Finally, a parametric study was carried out on the concentration of fixed charges and applied potential.

Results

The simulation results showed that there is formate accumulation at the AEM/SSE boundary when the concentration of fixed charges is increased. Additionally, the anion distribution as well as the concentration of formate ions throughout the three-compartment electrolyzer domain increases when the applied potential and the concentration of fixed charges increase.

Conclusion

Future work is to simulate the concentration of protons reaching the central compartment by adding a proton exchange membrane at the anode compartment.

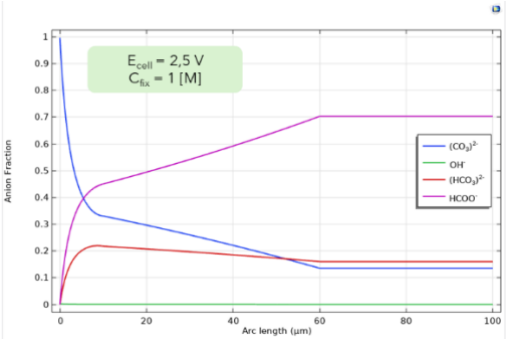

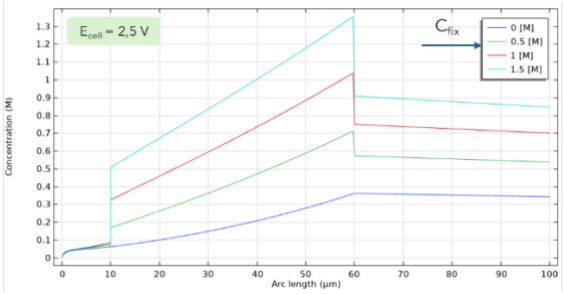

References

1. Lin, J., Zhang, Y., Xu, P. & Chen, L. CO2 electrolysis: Advances and challenges in electrocatalyst engineering and reactor design. Materials Reports: Energy vol. **3** Preprint at https://doi.org/10.1016/j.matre.2023.100194 (2023).

2. Zhu, P. & Wang, H. High-purity and high-concentration liquid fuels through CO2 electroreduction. Nature Catalysis vol. **4** 943–951 Preprint at https://doi.org/10.1038/s41929-021-00694-y (2021).

3. Fan, L., Xia, C., Zhu, P., Lu, Y. & Wang, H. Electrochemical CO2 reduction to high-concentration pure formic acid solutions in an all-solid-state reactor. Nat Commun **11**, (2020).

4. Xia, C. et al. Continuous production of pure liquid fuel solutions via electrocatalytic CO2 reduction using solid-electrolyte devices. Nat Energy **4**, 776–785 (2019).

Modeling of Electrodialytic Desalination of Wastewater Effluent

Elena Olivares-Ligero[1,2], María Villén-Guzmán[2], María J. Martínez-Salverri[1], Juan A. Baez Durán[3], José M. Rodríguez-Maroto[2], María M. Cerrillo-González[2] y Juan M. Paz-García[2*]

[1]SANDO AGUA, Calle la Bohéme 40, 29006 Malaga (Spain)
[2]Departament of Chemical Engineering, University of Malaga (Spain)
[3]SANDO, Calle Ortega y Gasset 112, 29006 Málaga (Spain)
*Corresponding author: juanma.paz@uma.es

Introduction

Electrodialytic desalination (EDD) is a promising method for wastewater treatment. In EDD, an electric field drives the movement of ions through ion-exchange membranes, effectively removing salts and other impurities from water. This process has already been utilized to produce water suitable for drinking and agricultural purposes. Unlike traditional methods such as reverse osmosis, electrodialysis offers lower energy consumption and reduced chemical usage.

A model for EDD of brackish wastewater has been developed. The objective of EDD is to reduce the conductivity of the water to levels suitable for agricultural use in a single pass through the membrane system. Additionally, the cell is designed to ensure that the separated ions generate valuable solutions in the electrode compartments. Specifically, a four-compartment cell has been conceptualized to avoid chlorine gas formation at the anode, producing HCl and NaOH-rich solutions along with the diluted stream.

Use of COMSOL Multiphysics

A 2D Tertiary Current Distribution (TCD) model has been implemented to simulate an electrodialytic cell with four compartments. From left to right, the compartments are: (1) the anode and anolyte compartment, (2) the HCl concentration compartment, (3) the wastewater treatment compartment, and (4) the cathode and catholyte compartment. An anion-exchange membrane and a cation-exchange membrane are placed on the left and right sides of compartment 3, respectively. Additionally, a cation-exchange membrane is positioned between compartments 1 and 2 to prevent chloride ions from reaching the anode and producing chlorine gas. Figure 1 shows a schematic of the cell design.

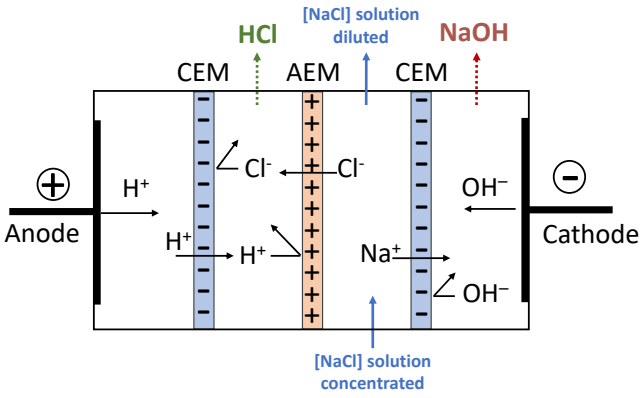

Figure 1. Schematics of a four-compartment EDD cell

The TCD model is solved considering the electroneutrality condition. Donnan boundary conditions are applied at each side of the ion-exchange membranes, which are modeled as thin porous media with a fixed structural ionic charge. This detailed approach ensures accurate simulation of ion transport and electrochemical behavior within the electrodialytic cell.

Results

By adjusting concentration of inflows, applied electrical current and the flow rate of the different channels, it is possible to optimize the desalination process and the energy consumption. Results showed efficient NaCl concentration reduction in the wastewater effluent, and concentration of valuable HCl and NaOH solutions in the collecting compartments. In order to enhance reliability, the model was adjusted to work using chemical equilibrium reactions modeled as very fast reversible reactions. In particular, water self-ionization was included in the model to monitor the corresponding acid and basic fronts generated at the anode and the cathode.

Conclusion

The implemented model has demonstrated the theoretical feasibility of the technique and has been used for optimizing the cell geometry and fluid dynamics conditions to maximize the production of desired streams while minimizing energy consumption in lab-scale experiments.

Future work will focus on validating the model with experimental data using actual wastewater effluent. Once validated, the model will be employed to design a pilot-scale cell for the desalination of high-conductivity wastewater effluent. The ultimate goal is to develop a technique capable of conditioning wastewater effluent for agricultural use in the Costa del Sol region, thereby helping to alleviate water stress in the area.

References

1. Cerrillo-Gonzalez, M.D.M., Villen-Guzman, M., Rodriguez-Maroto, J.M., Paz-Garcia, J.M., Metal Recovery from Wastewater Using Electrodialysis Separation, *Metals*, **14**, 38 (2024).
2. C. Magro, J. Almeida, J.M. Paz-Garcia, E.P. Mateus, A.B. Ribeiro, *Electrokinetic Remediation for Environmental Security and Sustainability*. John Wiley and Sons Ltd., online (2021).

Iberian COMSOL Multiphysics CONFERENCE
Málaga. June 28, 2024

O6

A Simulation of the Spatial Distribution of Chemical Species During the Corrosion of the Zn-Fe Galvanic Couple

Alexandre Bastos*[1], Juan M.P. Garcia[2] y Emilio R. Reina[3]

[1]Department of Materials and Ceramic Engineering and CICECO – Aveiro Institute of Materials, 3810-193 Aveiro, Portugal,
[2]Department of Chemical Engineering, Facultad de Ciencias, Universidad de Malaga, Spain,
[3]Department of Applied Physics II, Escuela de Engenierias Industriales, Universidad de Malaga, Spain.
*Corresponding author: acbastos@ua.pt

Introduction

The zinc-iron galvanic coupling is of great importance for the corrosion protection of steel. Major examples are galvanised steel and the use of zinc anodes for the cathodic protection of naval ships and offshore structures.

This work presents a numerical simulation of the electrochemical processes and the associated distribution of chemical species taking place during the corrosion of the zinc-iron galvanic couple. A small electrochemical cell was constructed with separated zinc and iron electrodes, electrically connected from the back – Figure 1 a) and b). The spatial distribution of pH, dissolved O_2, electrical potential and ionic current density in aqueous NaCl solutions was monitored with microelectrodes. A finite element model was implemented using the experimental data to set the boundary conditions and initial values.

Use of COMSOL Multiphysics

Figure 1 c) shows the model geometry, corresponding to half of the cell, where the boundaries are: 1 (zinc electrode, anode), 2 (iron electrode, cathode), 3 (top, solution/air interface), 4 (symmetry plane) and 5 (side walls and epoxy mount surface). The mesh is presented in Figure 1 d). The model was set in COMSOL Multiphysics 5.6. using the *Tertiary Current Distribution, Nernst-Plank Interface* with the *Water-based with electroneutrality charge conservation* model. The simulation was made with a *Time dependent* study. The governing equations were the mass balance of each chemical species (Table 1 in Figure 2), the Nernst-Plank equation, and the electroneutrality maintained by the water ionization species, H^+ and OH^-.

The zinc and iron electrodes correspond to boundaries 1 and 2. The current density in each electrode was set by experimental polarization curves, added as interpolation functions in the materials (Zn and Fe) nodes. The top boundary (3) was the solution-air interface and allowed the normal flux of oxygen. The walls and the polymeric base (boundaries 5) were assumed to be insulating walls, with the normal fluxes of species and the current in solution set to zero. A symmetry boundary condition was assigned to boundary 4, with no flux properties. The values in Table 1 were set as Initial Values. A solution potential of $-E_{Zn}{}^0$ was also set as an initial value.

Results

Figure 2 b) shows the experimental and Figure 2 c) the simulated potential in solution established during the corrosion of the Zn-Fe galvanic corrosion. This potential is related to the ionic current

flowing in the cell, transported by all charged species in solution. The values are not very different, from -6 mV to 6 mV in the experiment and from 8.6 mV to -8.8 mV in the simulation.

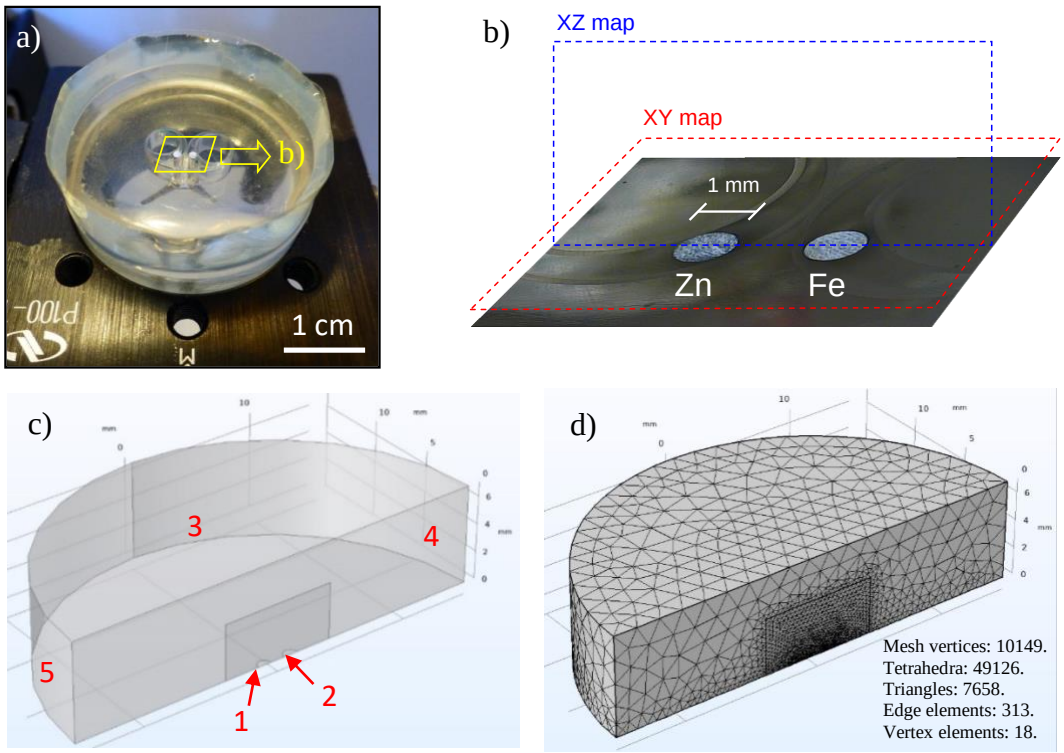

Figure 1: a) Zn-Fe electrochemical cell, b) position of the mapped areas with microelectrodes, c) model geometry, d) mesh used in the simulation.

One reason for the difference is that the experimental map starts 50 µm above the surface (to avoid breaking the glass microelectrode) missing the region of higher potential difference, which is in the vicinity of the electrodes' surfaces. The main difference between the maps is the point of zero potential, which is placed in the middle of the experimental map, while in the simulation most of the potential drop occurs in the vicinity of the anode (Zn).

The z component of the local current density (current normal to the electrode surface) was measured with a Scanning Vibrating Electrode Technique (SVET) and is presented in Figure 2 d). The calculated values (Figure 2 e)) are close to the experimental ones.

Conclusion

This model was capable of replicating most of the experimental observations. Improvements are expected when the model considers natural convection and homogenous chemical (precipitation) reactions. The model can be easily modified for studying the effect of geometry parameters (distance between electrodes, electrodes sizes, thickness of solution layer), the nature of the electrodes and type of electrolyte species.

a) Species considered in the model.

Species	c_i^0 (mol m^{-3})	z_i	D_i (x10^9 m^2 s^{-1})
O_2	0.23	0	1.96
Na^+	5	+1	1.2
Cl^-	5	-1	1.19
H^+	-	+1	9.31
OH^-	-	-1	5.26
Fe^{2+}	10^{-3}	+2	0.65
Zn^{2+}	10^{-3}	+2	0.7

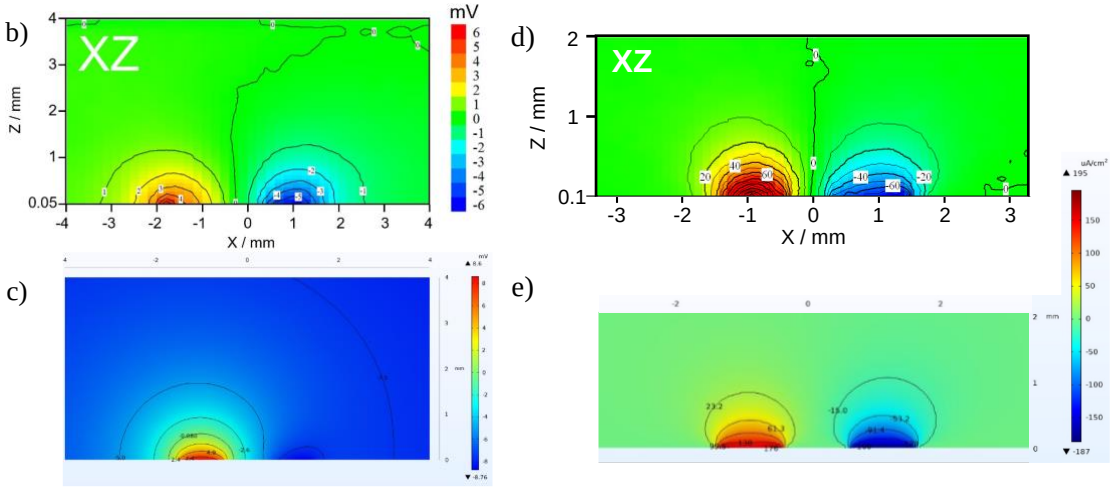

Figure 2: a) Species considered in the model, b) experimental results and c) numerical simulation, of the potential in solution (0.005 M NaCl) during the galvanic corrosion of the Zn-Fe couple, d) experimental results and e) numerical simulation, of the ionic current density in solution.

An Effective Simulation Framework for Fluid Flow in Microwave-Heated Packed Beds

Carlos González Niño*[1]

[1] Área de Industria y Energía, CIRCE Centro Tecnológico, Parque Empresarial Dinamiza, Avenida Ranillas, Edificio 3D, 1ª Planta. 50018, Zaragoza (España)
*Corresponding author: cgonzalez@fcirce.es

Introduction

Microwave heating presents a promising pathway for renewable and efficient heating processes, directly transferring heat into the core of matter. Nonetheless, certain materials -plastics targeted for pyrolysis in this case- exhibit limited susceptibility to this form of heating. Consequently, the employment of susceptor materials, such as silicon carbide (SiC), becomes imperative.
This study delves into the application of microwave heating within a packed bed configuration featuring SiC spheres, reducing computational workload while preserving the observed impact of electromagnetic field concentrations at tangent points between the spheres, a key feature of these systems noted in prior experimental investigations [1].

Use of COMSOL Multiphysics

The study starts by simulating in detail a small cubic segment of the packed bed under controlled conditions. Notably, the study distinguishes itself from others [2,3] by adopting realistic positioning of the spheres instead of using periodic ideal structures. To avoid errors importing overlapping spheres, an algorithm was developed that makes slight adjustments in the positioning of the spheres enabling their importation into COMSOL Multiphysics through Java scripting.

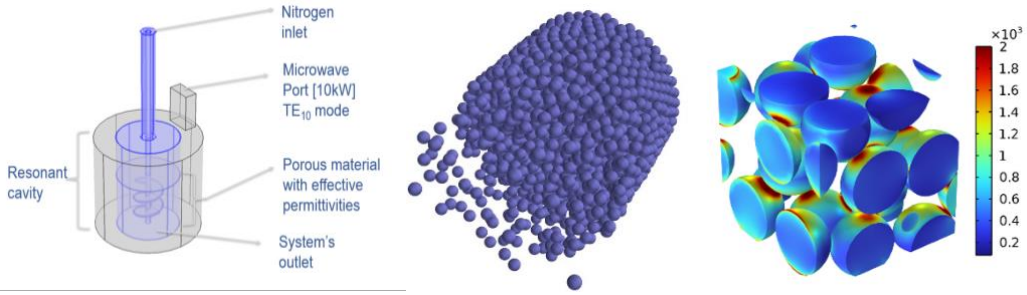

Figure 3: Schematic Representation of the MW Reactor (Left), Internal Perspective of the SiC Spheres (Center), and RF Simulation of a Small Cubic Segment Within the Spheres (Right).

Subsequently, an equivalent volume of homogeneous material is simulated and compared to the heterogeneous simulation results until two crucial metrics align: electromagnetic losses and stored electric energy. This is done via automation of the simulation, where a Nelder-Mead Simplex algorithm is used to vary both the real and imaginary parts of the permittivity of the effective material iteratively until the sum of the relative errors incurred in for Q_e and W_e is minimized. Notably, by using this approach the maximum error obtained by repeating this approach in the wide range of temperatures explored was of $9.62 \cdot 10^{-4}$%.

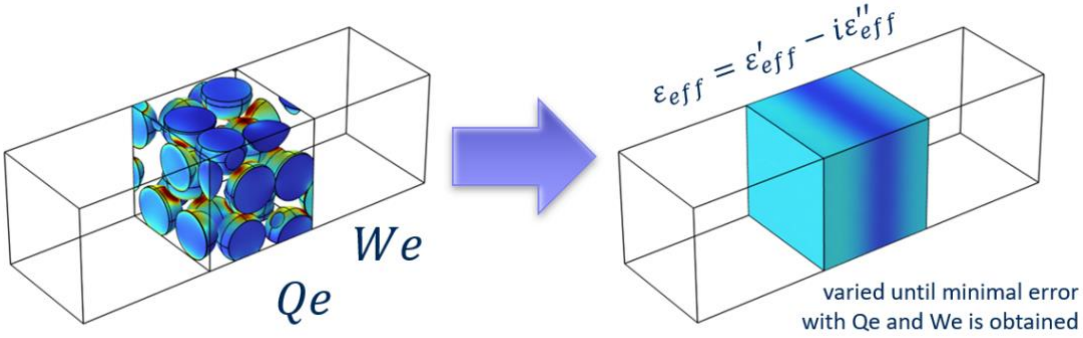

Figure 4: Conceptual Schematic Illustrating the Estimation of Effective Permittivity for an Equivalent Homogeneous Block.

These temperature-dependent permittivity values for the effective material were utilized in subsequent simulations. These multiphysics simulations integrated radiofrequency (RF), fluid flow dynamics, and heat transfer phenomena without the need to model thousands of individual spheres.

The Brinkman equations were used in the bulk of the porous material, for which the Forchheimer drag was calculated using known literature values for the Forchheimer coefficient and the permeability.

The heat transfer modeling accounts for the heat exchange between the spheres and the surrounding flow. This required user manipulation so that the electromagnetic losses are conceptually concentrated in the spheres.

Results

A visual summary of the findings is presented in the figure. The computational mesh utilized consisted of 577,278 elements, and the entire computation, which involved coupling all physics for a stationary solution, required 18 hours and 15 minutes to complete on a machine equipped with an AMD Ryzen 9 5950X 16-Core Processor.

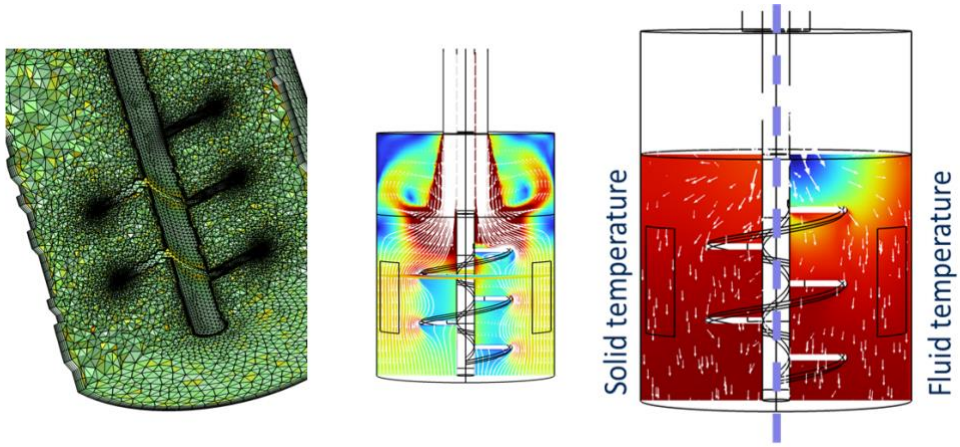

Figure 5: Mesh Configuration Employed (Left), Velocity Field and Fluid Streamlines (Center), and Temperature Distribution in the Solid and Fluid Phases within the Packed Bed (Right).

Conclusion

This study presents a novel approach that, to the best of the author's knowledge, allows for the simulation of fluid flow through a packed bed of microwave susceptors being heated for the first time. Modeling thousands of individual spheres is impractical due to the high computational and memory demands. The proposed methodology offers a promising solution to this challenge, providing a viable tool for microwave reactor design when packed bed susceptors are needed.

References

1. Haneishi, N. et al., Enhancement of Fixed-Bed Flow Reactions under Microwave Irradiation by Local Heating at the Vicinal Contact Points of Catalyst Particles, *Sci. Rep.*, **9**, 222 (2019).
2. R.M. Costa Mimoso, J.M. da Silva, and J.C. Fernandes, Computational Method for Calculating the Effective Permittivity of Complex Mixtures, *J. Microw. Power. Electromagn. Energy*. **49**, 2, 85-99 (2015).
3. H. Goyal, and D.G. Vlachos, Multiscale modeling of microwave-heated multiphase systems, *Chem. Eng J.*, **397**, 125262 (2020)

Iberian COMSOL Multiphysics CONFERENCE
Málaga. June 28, 2024

O8

Modelling and Simulation of a Packed Bed Adsorption column for edible oil decolorization.

Carlos Macías[1,2]*

[1] PROYMATICA 21 S.L
[2] CM Biolab 2020 S.L.
*Corresponding author: carlosmacias@cmbiolab.com, carlosmacias@proymatica21.com

Introduction

Oils extracted from some vegetal fruits, seeds or vegetal by products, must be refined prior to qualify as edible oils. Refining process comprises three steps which are common to all kind of crude oils: neutralization, decolorization and deodorization. Besides, some kinds of oils may require additional steps of dewaxing and degumming [1]. Decolorization is the removal of vegetal pigments from the oil. These pigments are usually chlorophylls and carotenoids and are removed by adsorption on 0.5-3% bleaching earths (BE) and also 1-5% of powder activated carbon (PAC) may be required in some cases. Decolorization is performed in batch reactors at 90-150 ºC and under mild vacuum. This is the most extended and standard technology but has the drawbacks of requiring downstream processing with special filters to separate the exhausted BE from the oil, a solid waste is generated in each batch with oil losses and due to the bleaching conditions, the oil suffers alterations in some oil quality parameters [2]. Besides, due to evolution of the raw material, chlorophylls evolve to pheophytins and pheophorbides [3] against which BE or PAC is not effective, giving oils with a deep brown color which must be sold as a lower quality non-edible oil. Packed bed adsorption column with porous silica, adsorbent resins and or granular activated carbon, is a promising alternative technology since it operates in continuous mode, at ambient temperature and pressure and the adsorption bed can be regenerated several times with solvents, lowering the treatment costs and oil losses and with the right media combination, it can remove any kind of pigments (figure 1). It has the drawback of using organic solvents like hexane, which are flammable and requires special anti-explosion facilities which are more capital expensive and have a higher complexity since they must be recovered through flash distillation and recycled back in the process. There is very scarce research done on this kind of processes and only restricted to lab-scale trials [4-6]. To best of my knowledge, there are no oil refining plants operating with this technology. Furthermore, there is no published research on mathematical models or simulation of this kind of processes in edible oils. At the time that this work is written, an industrial scale facility with this technology is being setup in an oil refining facility in Andalucía, Spain. In this work, a multyphysics model is proposed to simulate, test, dimensioning and optimization of fixed bed columns loaded with porous silica for pheophytins and pheophorbides removal from crude oils.

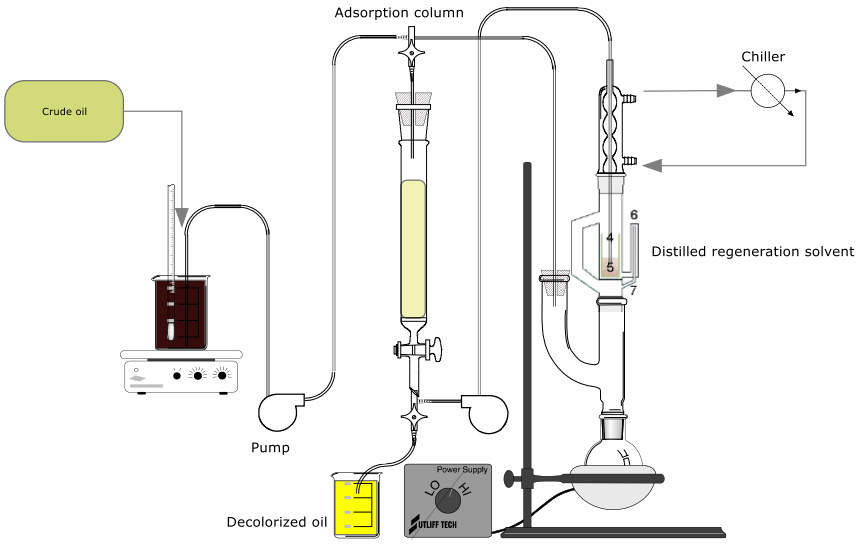

Figure 1: Bench scale set up of the fixed bed oil decolorization technology

Use of COMSOL Multiphysics

For the present work, the transport of diluted species (tds) in porous media module of COMSOL Multiphysics has been used to satisfactorily simulate the process. The tds module implements a Porous Medium feature including fluid and porous matrix features with diffusion and porosity experimental values and an adsorption feature with a Freundlich adsorption isotherm with parameters adjusted to experimental results.

Results

Figure 2 shows the breakthrough curve of the decolorization column as a function of the bed volume under real operation conditions. This plot is needed for the dimensioning of the real column.

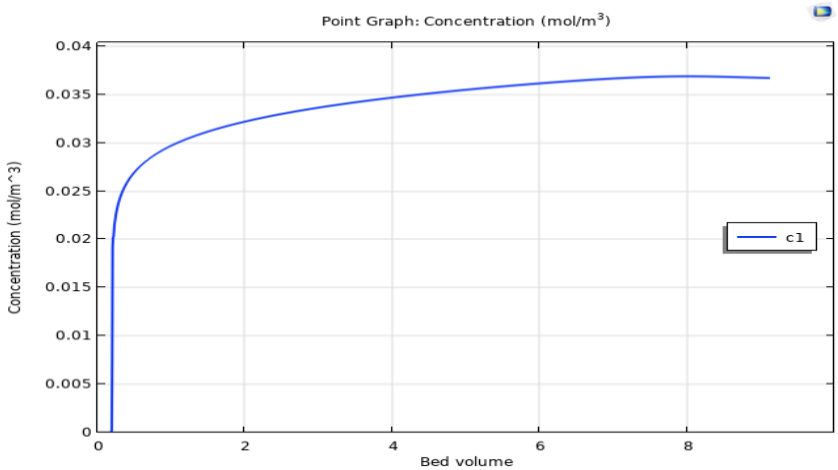

Figure 2: Breakthrough curve of pigment concentration vs bed volumes

Conclusion

The present study shows that multiphysics simulation is a useful tool for the analysis and rational design of column extraction and separation processes with adsorption, advection and diffusion phenomena. With this multiphysiscs modeling and simulation it can be proven that the real column has been correctly dimensioned.

References

1. De Greyt, W. and Kellens M. Refining Practice. Edible Oil processing. 90-105 Sheffield Academic Press UK (2000).

2. Amati. A, Minguzzi, A. and Losi G. Bleaching of Olive Oils. I. Variations in some physisco-chemical as a function of operation conditions. Riv. Ital. Sostanze Grasse **46**, 73-79 (1969).

3. Ofelia B. O. Ashton, Marie Wong, Tony K. Mcghie, Rosheila Vather, Yan Wang, Cecilia Requejo-Jackman, Padmaja Ramankutty and Allan B. Woolf. Pigments in Avocado Tissue and Oil. J. Agric. Food Chem. **54**, 10151-10158 (2006)

4. Bogdanor, J.M., and Price, A.L. Novel Sinthetic Silica Adsorbents for refining Edible Oils. Oil Mill Gazzeteer **99** 32–34 (1994).

5. Ihsan Karabulut, Ali Topcu, Canan Akmil-Basar. Obtaining Butter Oil Triacylglycerols Free from b-Carotene and a-Tocopherol via Activated Carbon Adsorption and Alumina-Column Chromatography Treatments. J. Am. Oil. Chem. Soc. **85** 213–219 (2008).

6. Abrehem Abad and Fereidoon Shahidi. A robust stripping method for the removal of minor components from edible oils. Food Production Processing and Nutrition. **2**, 1-9 (2020).

Multiphysics Modeling of Microwave Technology for Sustainable Revalorization of Metal Casting Molding Sands

P. Garcia-Michelena*[1], I. Crespo[2], G. Arruebarrena[1], I. Vicario[2], X. Chamorro[1], I. Hurtado[1].

[1]Mechanical and Manufacturing Department, Mondragon University.
[2]TECNALIA, Basque Research and Technology Alliance (BRTA).
*Corresponding author: pgarciam@mondragon.edu

Introduction

Casting is a widely used method for manufacturing metal components, but it has a substantial environmental impact due to high energy and material requirements [1]. Sand casting, in particular, produces large amounts of contaminated waste, especially used sand from molds and cores [2]. This quartz sand mainly consists of silica and chemical additives such as resins and binders accounting approximately for the 5% of the sand [3]. Currently, disposed sand is recovered by heating up to 800 ºC to evaporate resins and binders, a method that is both energy-intensive and time-consuming. Therefore, there is a demanding need for cleaner and more efficient technologies for sand revalorization [4]. This study explores the feasibility of using microwave radiation to revalorize disposed foundry mold sands.

Use of COMSOL Multiphysics

A multiphysics model was developed using COMSOL Multiphysics® v6.0 to simulate the dielectric heating of a mixture of silica and Furan-based resin by microwave radiation. On a macroscopic scale, a three-dimensional geometry was developed coupling the dissipation of the electrical field in the sand as heat and the resulting transient temperature increase. The resonant cavity, designed to emulate a conventional microwave furnace, utilized the Port boundary condition of the Radio Frequency module to act as the magnetron, emitting a 2.45 GHz electromagnetic wave. This wave generates an electric field in the domain that induced a voltage potential in the sand and binder mixture, leading to dielectric heating. The dielectric properties of the sand, including real permittivity and loss factor were characterized up to 800 ºC. A sample of 200 g of sand with residual furan resin from foundry molds was used for validation. To manage the high temperatures, the sample was contained in an alumina-based crucible. The frequency domain study showed the electric field distribution within the furnace (Figure 1) and a significant concentration of the electric field was observed in the sand domain.

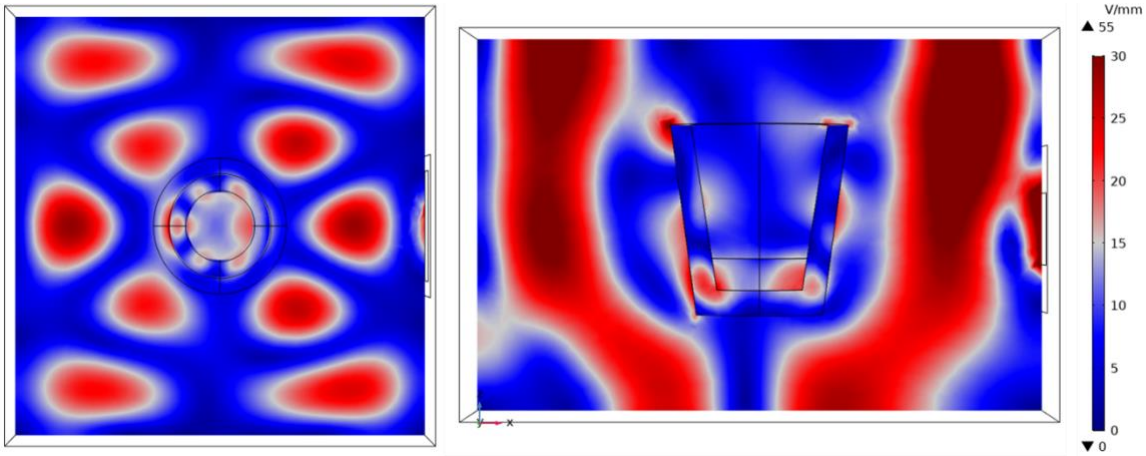

Figure 6: Electric field distribution in the microwave radiation sand recovery furnace.

In the thermal submodel, based on the Heat Transfer module, a coupled frequency-transient simulation was conducted. At each iteration, the electric field was recalculated, and the dielectric loss values were updated. As boundary conditions Radiation heat losses on the sand top surface and natural convection around the crucible were considered.

Results

The transient temperature evolution and distribution within the sand samples were compared with a heating test curve provided by TECNALIA. The model reproduced the temperature increment slope and the maximum temperature at the load's top contour matched, even the average temperature was slightly higher (Figure 2.a). The temperature reached 630 ºC in the contact zone with the crucible, while the upper surface was at 500 ºC, consistent with pyrometer measurements. Higher temperatures below the first sand layer were observed due to radiation heat losses from the top surface and the localized effect of the electric field (Figure 2.b).

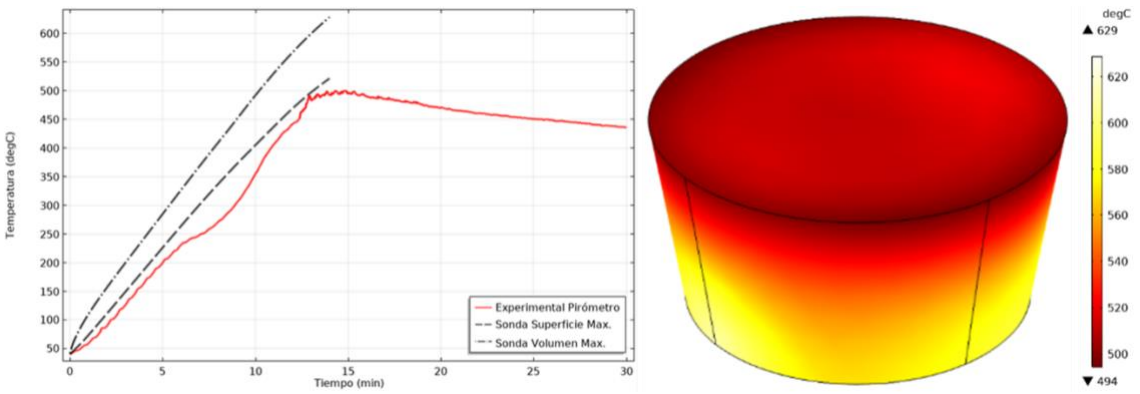

Figure 7: a) Transient numerical and experimental correlation of MW heating. b) Temperature of heated sand sample.

Conclusion

The simulations and experimental results showed that microwave radiation successfully induces significant dielectric heating within the sand mixture. The electric field distribution indicated areas of high intensity, leading to rapid temperature increases. Microwave radiation is a promising

technology for the revalorization of disposed sands and further studies could help in scaling up this technology for industrial applications.

References

1. M. Holtzer, R. Danko, and S. Zymankowska-Kumon, Foundry Industry. Current State and Future Development, Metalurgija, vol. 51, pp. 337–340, (2012).
2. M. K. Joseph, F. Banganayi, and D. Oyombo, Moulding Sand Recycling and Reuse in Small Foundries, Procedia Manufacturing., vol. **7**, pp. 86–91, (2017).
3. M. Holtzer, R. Dańko, and A. Kmita, Influence of a Reclaimed Sand Addition to Moulding Sand with Furan Resin on Its Impact on the Environment, Water. Air. Soil Pollut., vol. **227**, pp. 1–12, (2016).
4. J. Dañko, R. Dañko, and M. Holtzer, Reclamation of used Sands in Foundry, Metalurgija, vol. **42**, pp. 173–177, (2003).

Nonlinear Dependence of Flow Velocity in Electrothermoplasmonics with Gold Nanoparticles Suspension

Carlos David González-Gómez[*1,2], Raúl A. Rica[2] y Emilio Ruiz-Reina[1]

[1]Department of Applied Physics II, Universidad de Málaga, 29071, Málaga Spain,
[2]Nanoparticles Trapping Laboratory, Department of Applied Physics, Universidad de Granada, 18071, Granada, Spain
*Corresponding author: cdgg@uma.es

Introduction

In recent years, lab-on-a-chip devices are gaining popularity in many fields [1,2]. Nevertheless, fluid flow generation in the microscale is still a hurdle that has to be optimized [3]. Here, we present a novel technique that combines an AC electric field with a small temperature gradient, which leads to a strong electrothermal flow. This effect is known as electrothermoplasmonic flow [4,5]. We performed experiments and simulations with COMSOL Multiphysics to characterize this effect.

Use of COMSOL Multiphysics

We performed simulations in COMSOL Multiphysics to model the flow field (see Fig. 1 a)) produced by the combination of the AC electric field and the small temperature gradient. To so, we used the Fluid Flow and Heat Transfer in Fluids and Solids physics interfaces.
In a different model, we also performed electromagnetic simulations using Electromagnetic Waves, Frequency Domain physics interface to estimate the absorption cross-section of the gold nanoparticles and to detect the possible presence of aggregates in the sample used.

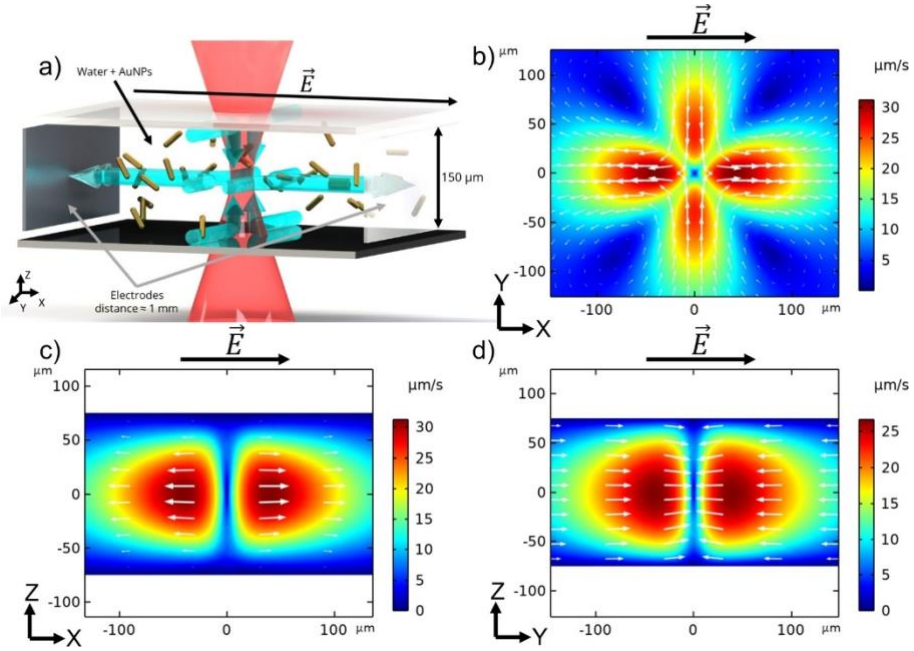

Figure 8: a) Schematic representation of the microchamber. Panels b), c) and d) show the simulated flow fields in the XY, XZ and YZ planes, respectively.

Results

In Fig. 1 b), c) and d) we show the simulated flow field in Z, Y and X planes, respectively. As we note, the flow field goes outwards from the focal point of the laser when the electric field is applied in that direction and flows inwards in all other directions.

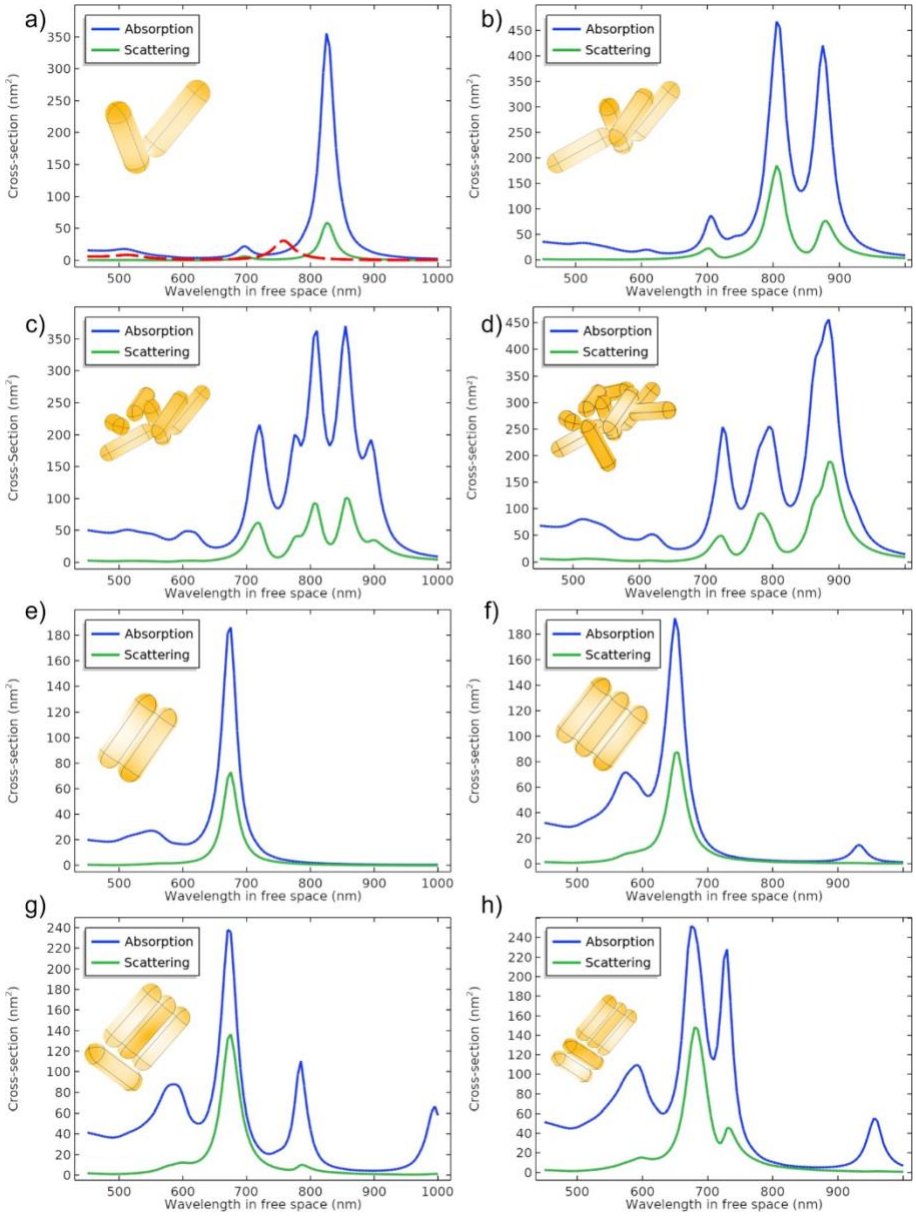

Figure 9: Absorption and scattering cross-sections for random aggregates of a) 2 nanoparticles,b) 4 nanoparticles, c) 6 nanoparticles, and d) 9 nanoparticles. Also, the absorption and scattering cross-sections for orderly distributed aggregates of e) 2 nanoparticles, f) 3 nanoparticles, g) 4 nanoparticles, and h) 5 nanoparticles.

In panels a)-d) of Fig. 2 we present the simulated results of absorption and scattering cross-sections for random aggregates of 2, 4, 6 and 9 nanoparticles, respectively. Also, we show in panels e)-h) the simulated results of absorption and scattering cross-sections for orderly distributed aggregates of 2, 3, 4 and 5 nanoparticles, respectively.

Conclusion

We were able to simulate the electrothermoplasmonic flow in the chamber. The shape of the simulated flow field is in good agreement with the experimental flow field. More work is needed to model the second order relationship between the gold nanoparticles concentration and the maximum velocity achieved.

Also, thanks to the electromagnetic simulations, we detected the presence of particle aggregation in our solution. Further work is required to understand better the type of aggregation present in the sample used.

Acknowledgements

The authors thank Grant No. PID2021-127427NB-I00 funded by MCIN/AEI/10.13039/501100011033 and by "ERDF A way of making Europe"

References

1. A. Hatch et al., Diffusion-based analysis of molecular interactions in microfluidic devices, *Proc. IEEE*, 92 (**1**), 126-139 (2004).

2. T.M. Squires et al., Making it stick: convection, reaction and diffusion in surface-based biosensors, *Nat. Biotechnol.*, 26 (**4**), 417-426 (2008).

3. T.M. Squires et al., Microfluidics: fluid physics at the nanoliter scale., *Rev. Mod. Phys.*, 77 (**3**), 977 (2005).

4. J. Garcia-Guirado et al., Overcoming diffusion-limited biosensing by electro-thermo-plasmonics, *ACS Photonics*, **5**, 3673-3679 (2018).

5. C. D. González-Gómez et al., Electrothermoplasmonic flow in gold nanoparticles suspensions: Nonlinear dependence of flow velocity on aggregate concentration, *Journal of Colloid and Interface Science*, **648**, 397-405 (2023).

Iberian COMSOL Multiphysics CONFERENCE
Málaga. June 28, 2024

O11

Modeling of an Acoustic Leaky-Wave Antenna for Spatial Localization

Alejandro Fernández-Garrido*[1], María Campo-Valera[2], Elena Abdo-Sánchez[2], Rubén Picó[3] and Rafael Asorey-Cacheda[1]

[1]Departament of Information and Communication Technologies, Universidad Politécnica de Cartagena,
[2]Telecommunication Research Institute (TELMA), Universidad de Málaga,
[3]Institut d'Investigació per a la Gestió Integrada de les Zones Costaneres (IGIC), Universitat Politècnica de València.
*Corresponding author: alejandro.fernandez3@upct.es

Introduction

The use of acoustic signals to locate objects in space has evolved significantly, highlighting techniques such as SONAR. An innovative alternative are Acoustic Leaky-Wave Antennas (ALWAs), which, inspired by electromagnetic Leaky-Waves Antennas (LWAs), uses a single transducer to emit directional beams by changing the operating frequency, offering a low cost and low power consumption solution for acoustic localization applications [1][2][3].
This paper presents a numerical model of an ALWA to determine its radiation patterns, the reflection and transmission coefficients. The results are obtained using specific boundary conditions.

Use of COMSOL Multiphysics

To model the problem, a 2D axisymmetric dimension is used due to the geometry's axial symmetry. The physics of *Pressure Acoustics* is applied, and a *Frequency Domain* study is conducted. The geometry, as shown in Figure 1a, consists of three parts: the first two are waveguides of radius r_{wg} an input length l_{wgIn} and an output length l_{wgOut}. The third part is a periodic region between them formed by 32 disk-shaped cells with a thickness of t_{cell} and arranged side by side with a separation of w_{sh}. As for the frequency of interest and meshing, as shown in Figure 1b, quadratic meshing is used due to the rectangular shape of the different parts that compose the geometry in 2D. A frequency sweep is performed from $10\ Hz$ to $10\ kHz$ in $10\ Hz$ steps. For each frequency, the mesh is discretized as $\Delta x = \lambda/n$, where $n = 10$ and λ at the maximum operating frequency. The boundary conditions used include ports for excitation and measurement of physical fields, narrow region acoustics models for layer-induced losses, perfectly matched boundaries to absorb incident waves and external field calculation to obtain information on acoustic pressure outside the study area.

Results

The radiation pattern and the transmission and reflection coefficients of the ALWA are obtained for different excitation frequencies. Figure 2a shows the radiation patterns. The antenna beam scanning is observed with changes in the excitation frequency. Figure 2b, shows the transmission coefficient (T), where the red curve represents the proportion of the wave that is transmitted from the input waveguide to the output waveguide. The blue curve shows the reflection coefficient (R) which measures the proportion of the wave that is reflected in the same input waveguide. As the

waveguide is propagating the acoustic wave at the operating frequency (2700 Hz), it is observed an increase in the transmission coefficient and decrease in the reflection one. The leakage of power along the structure in form of radiation is demonstrated since, although not having reflections in the operating band, the transmission coefficient is far from 1.

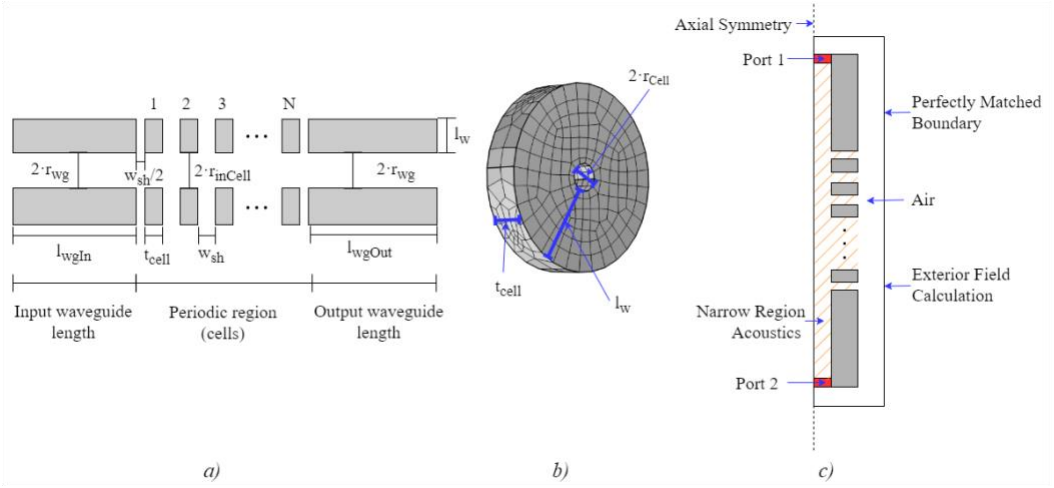

Figure 1: ALWA geometry presented. a) Parameters geometry, b) mesh, c) boundary conditions of the antenna design.

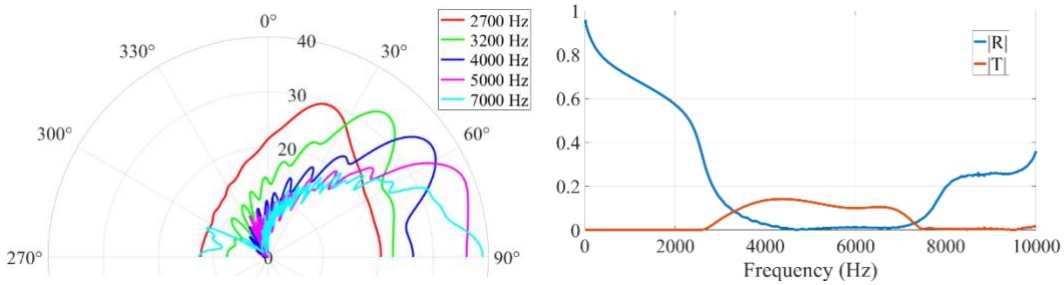

a) **b)**

Figure 2: Simulations results. a) Radiation patterns, b) transmission (T) and reflection (R) coefficients.

Conclusion

Numerical simulation of the ALWA with COMSOL Multiphysics allowed to obtain the directivity and the transmission and reflection coefficients. The ability of this type of antenna to scan the radiation beam by changing the working excitation frequency was demonstrated, making it useful for source localization.

Acknowledgements

This work was the result of the ThinkInAzul and AgroAlNext programmes, funded by Ministerio de Ciencia, Innovación y Universidades (MICIU) with funding from European Union NextGenerationEU/PRTR-C17.I1 and by Fundación Séneca with funding from Comunidad Autónoma Región de Murcia (CARM). This work was also supported by the grants PID2020-116329GB-C22 and TED2021-129336B-I00, funded by MICIU/AEI/10.13039/501100011033 and by the European Union NextGenerationEU/PRTR. This work was also funded by Fundación Séneca (22236/PDC/23).

References

1. C. J. Naify, M. Haberman, M. D. Guild, and C. F. Sieck, "Acoustic Leaky Wave Antennas: Direction-Finding via Dispersion," *Acoustic Today*, vol. **14**, pp. 31–38, 2018.
2. Qi Wang, Jun Lan, Zhaoyu Deng, Yun Lai, Xiaozhou Liu; Acoustic source localization based on acoustic leaky-wave antenna with heterogeneous structure. *J. Acoust. Soc. Am.* **153** (1): 487–495. 1 January 2023, doi: 10.1121/10.0016815.
3. C. W. Broadman, C. J. Naify, M. J. Lee, and M. R. Haberman, "Design of a one-dimensional underwater acoustic leaky wave antenna using an elastic metamaterial waveguide," *J Appl Phys*, **129**(19) p. 194902, May 2021, doi: 10.1063/5.0044802.

Iberian COMSOL Multiphysics CONFERENCE
Málaga. June 28, 2024

O12

Surrogate Modeling Applied to Solar Cell Performance Analysis Using COMSOL Multiphysics

Pablo Ferrada[1], Alejandro Cifuentes[2], Benjamin Ivorra[3]

[1]Department of Mathematical Analysis and Applied Mathematics, Complutense University of Madrid,
[2]Multiphysics Modeling School, Escuela de Ingenierías Industriales, Universidad de Málaga,
[3]Department of Mathematical Analysis and Applied Mathematics, Complutense University of Madrid
*Corresponding author: pferrada@ucm.es

Surrogate modeling has emerged as a valuable technique for optimizing complex systems, particularly in the realm of renewable energy technologies such as solar cells. This paper investigates the application of surrogate models in enhancing the performance of solar cells, with a focus on leveraging the computational capabilities of COMSOL Multiphysics.

The semiconductor module within COMSOL Multiphysics was used to create a detailed solar cell model. This model enables the computation of current-voltage (JV) characteristics for optimizing the device's output power (Fig. 1). However, the conventional optimization process can be time-consuming due to its reliance on physics-based models [1]. To streamline this process, a surrogate model was developed to complement the optimization efforts. This surrogate model efficiently computes responses to varying solar spectra and material parameters, offering an alternative to traditional physics-based approaches.

Through the integration of numerical simulations and machine learning techniques, surrogate models are developed to approximate the complex relationship between input parameters and solar cell performance metrics. These surrogate models demonstrate high accuracy in predicting solar cell efficiency, output power, and spectral response, as validated against additional simulation data. Furthermore, the efficiency of surrogate models in optimizing solar cell designs is showcased, with rapid exploration of the design space yielding configurations that maximize performance within practical constraints.

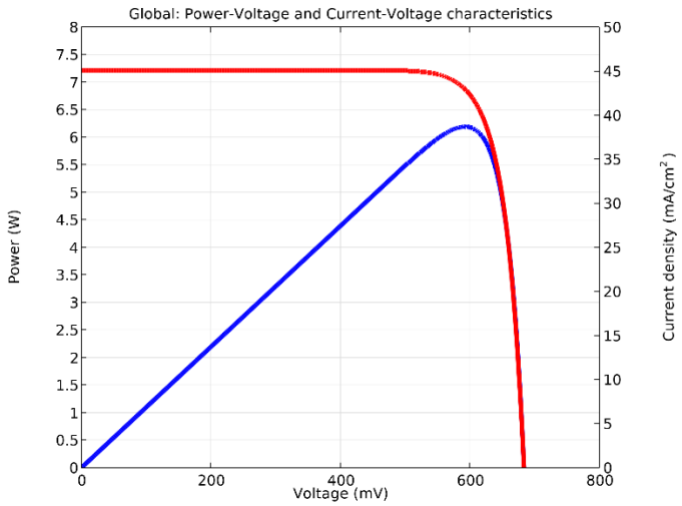

Figure 1: Current-Voltage curve of the solar cell.

The utilization of surrogate modeling within the COMSOL Multiphysics environment offers a promising avenue for accelerating the analysis and optimization of solar cell performance. By providing efficient approximations of computationally intensive simulations, surrogate models enable expedite the design process and identify optimal configurations. This study highlights the significance of surrogate modeling as a valuable tool for advancing solar cell technologies, ultimately contributing to the evolution of sustainable energy generation.

References

1. Pablo Ferrada, Aitor Marzo, Miriam Ruiz Ferrández, Emilio Ruiz Reina, Benjamín Ivorra, Jonathan Correa-Puerta, Valeria del Campo. Optimization of N-PERT Solar Cell under Atacama Desert Solar Spectrum. *Nanomaterials*, **12**(20), 3554 (2022).

Iberian COMSOL Multiphysics CONFERENCE
Málaga. June 28, 2024

O13

Acoustic Metamolecule Made of Eight Nanopillars Mediated by Surface Waves: High-Quality Resonances

Ricardo Martín Abraham-Ekeroth[*1-3], Liangshu He[4], and Dani Torrent[*1]

[1]Grup de Recerca Óptica de Castelló (GROC), Institut de Noves Tecnologies de la Imatge (INIT), Universitat Jaume I (UJI), Av. Vicent Sos Baynat s/n, 12071 Castelló de la Plana, Spain
[2]Instituto de Física Arroyo Seco (IFAS), Pinto 399, 7000 Tandil, Argentina.
[3]Centro de Investigaciones en Física e Ingeniería del Centro de la Provincia de Buenos Aires (UNCPBA-CICPBA-CONICET), Arroyo Seco s/n, 7000 Tandil, Argentina.
[4] University of Tongji, School of Aerospace Engineering and Applied Mechanics, No. 1239 Siping Road, 200092, Shanghai, China
*Corresponding author: abraham@uji.es, dtorrent@uji.es

Introduction

Multifield couplers in nanoscale structures are very useful for many applications today, thanks to the ability researchers have gained to fabricate and explore such devices. In particular, GHz acousto-optic control of waves has become essential since all communications based on compact devices can operate in this range [1]. Although faster technologies are on the horizon, modern electronic circuits have a processing speed in the same range. Thus, other types of wave-matter couplers and transducers are needed [2,3].

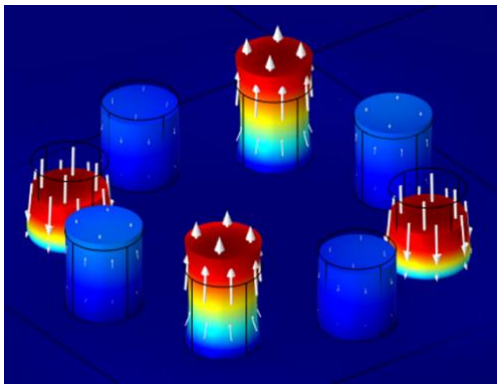

In this work, we study the concept of an acoustic molecule [4,5], a device capable of creating definite bound acoustic states that can interact with external fields in dissipative media. Specifically, we calculate the first eigenmodes and excitation frequencies of a circular array of eight elastic pillars made of SU8 photoresist, which are placed on top of a LiNbO3 128º Y-cut anisotropic plate [6], designed to operate around the GHz range.

Use of COMSOL Multiphysics

We perform simulations using COMSOL Multiphysics (version 6.2) with the Solid Mechanics interface of the Structural Mechanics Module, adding Eigenfrequency and Frequency Domain studies. PML layers were added to prevent back reflections to the physical domains.

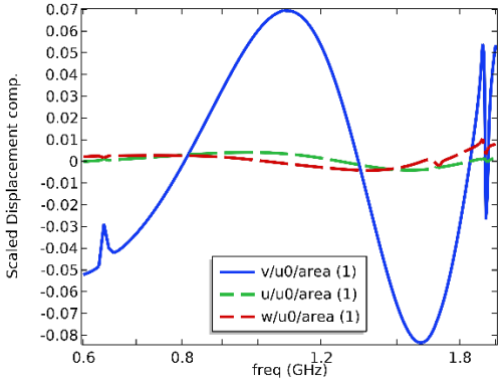

Results

We found that the possible acoustic states are weakly coupled from the perspective of excitation energies, as their frequencies split slightly and only when the pillars are too close to each other. However, their modal shapes demonstrate that the modes remain coupled and sensitive to symmetry in

the near field. These states correspond to evanescent waves traveling along the pillars due to single-pillar state hybridization, which resemble some molecular states in ordinary or photonic matter. On the other hand, we assess the quality of the resonances and find their response under external sources. Interestingly, the device converts polarization. A few resonances can even be considered as quasi-bound states in the continuum and show Fano line shapes in the spectra.

Conclusion

Our results may be helpful in the design of acousto-optic modulators, signal processing, cavity acoustic resonators, polarization conversion, and control/manipulation of acoustic waves using metamaterials.

References

1. Otsuka P H, Mezil S, Matsuda O, Tomoda M, Maznev A A, Gan T, Fang N, Boechler N, Gusev V E and Wright O B, Time-domain imaging of gigahertz surface waves on an acoustic metamaterial New J. Phys. 20 013026 (2018)

2. Muhammad, Lim C W, Reddy J N, Carrera E, Xu X and Zhou Z, Surface elastic waves whispering gallery modes based subwavelength tunable waveguide and cavity modes of the phononic crystals, Mechanics of Advanced Materials and Structures (2020)

3. Jin Y, Bonello B, Moiseyenko R P, Pennec Y, Boyko O and Djafari-Rouhani B, Pillar-type acoustic metasurface, Phys. Rev. B 96 104311, (2017)

4. Wang Y, Dong Y, Zhai S, Ding C, Luo C and Zhao X, Reconfigurable topological transition in acoustic metamaterials, Phys. Rev. B 102 174107 (2020)

5. Song H, Ding X, Cui Z and Hu H, Research Progress and Development Trends of Acoustic Metamaterials, Molecules 26 4018 (2021)

6. Weis R S and Gaylord T K, Lithium niobate: Summary of physical properties and crystal structure, Appl. Phys. A 37 191–203 (1985)

Iberian COMSOL Multiphysics CONFERENCE
Málaga. June 28, 2024

O14

Elastocaloric Effect at the Nanoscale in Cu–Al–Ni Shape Memory Alloys Modeled with COMSOL Multiphysics

Jose Fernando Gómez Cortés*[1], Emilio Ruiz Reina[2], Ed. González[3], María Luisa Nó[1] and Jose Maria San Juan[1]

[1]Departament of Physics, University of Basque Country (Spain),
[2]Department of Applied Physics II, University of Malaga (Spain),
[3]COMSOL AB (Sweden)
*Corresponding author: josefernando.gomez@ehu.eus

Introduction

The elastocaloric effect (eCe) is a groundbreaking solid-state technology for the refrigeration industry [1,2]. It offers a more efficient and environmentally friendly solution than conventional vapor-compression devices and provides practical solutions to modern micro-spot refrigeration challenges [3,4]. Shape memory alloys (SMAs) are active materials that exhibit a notable eCe, making them protagonist actors for the new solid-state refrigeration [1-4]. These alloys are "smart" materials due to their unique thermo-mechanical properties. One such property is the shape memory effect (SME), which allows them to return to a specific shape when heated. Another property is the superelastic effect (SE), which enables them to stretch significantly when a force is applied and return to their original shape when withdrawn. The SE is coupled to the eCe through a stress-induced martensitic transformation, as illustrated by the cycle in Figure 1A. 1→2: The austenite phase undergoes an exothermic stress-induced martensitic transformation. 2→3: Latent heat release. 3→4: The martensite phase reverse endothermic transformation. 4→1: Latent heat absorption. This thermo-mechanical behavior leads to a hysteresis superelastic cycle in the stress-strain field. It can be measured at the nanoscale through nano-compression experiments, showing promising results in Cu-based SMAs [5, 6]. Figure 1 B illustrates a nano-compression experiment on a pillar. A sphero-conical punch applies a mechanical field on the top of the pillar while force and displacement are measured simultaneously. Figure 1C shows a micrograph of a pillar tested in nano-compression, while Figure 1D illustrates its hysteretic superelastic behavior. This work aims to develop a thermo-mechanical model that describes a nano-compression experiment on a Cu-Al-Ni SMA pillar. The objective is to advance elastocaloric effect studies at the nanoscale for future micro/nano-spot refrigeration engineering.

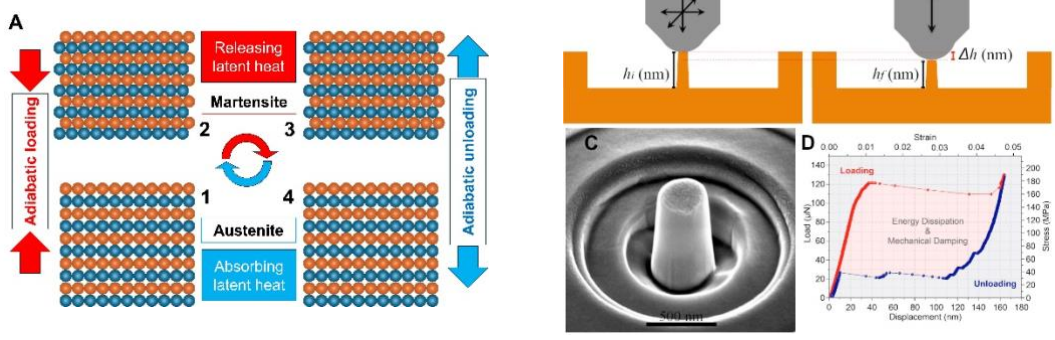

Figure 1: A) Illustration of the thermo-mechanical coupling in a stress-induced martensitic transformation cycle. B) Scheme of a nano-compression test. C) Scanning electron image of a micropillar. D) Superelastic response of the pillar to a nano-compression test.

Use of COMSOL Multiphysics

The thermo-mechanical model integrates the Souza-Auricchio shape memory material model within COMSOL Multiphysics, facilitating the coupling of solid mechanics and heat transfer in solids physics interfaces using a time-dependent model. Additional information regarding the geometry, material construction, and solver characteristics will be provided.

Results

We have developed a COMSOL Multiphysics model to simulate a nano-compression test on Cu-Al-Ni pillars. This model offers a comprehensive understanding of the superelastic behavior of this shape memory alloy (SMA), including all relevant mechanical and thermal information. The simulation covers applying micro loads and observing nanometric displacements and elastic and thermal responses, enabling a precise assessment of material properties under controlled conditions. Figure 2 A) shows the pillar geometry with the Von Mises stresses. Figure 2 B) depicts the superelastic behavior modeled in correlation with the martensitic volume fraction.

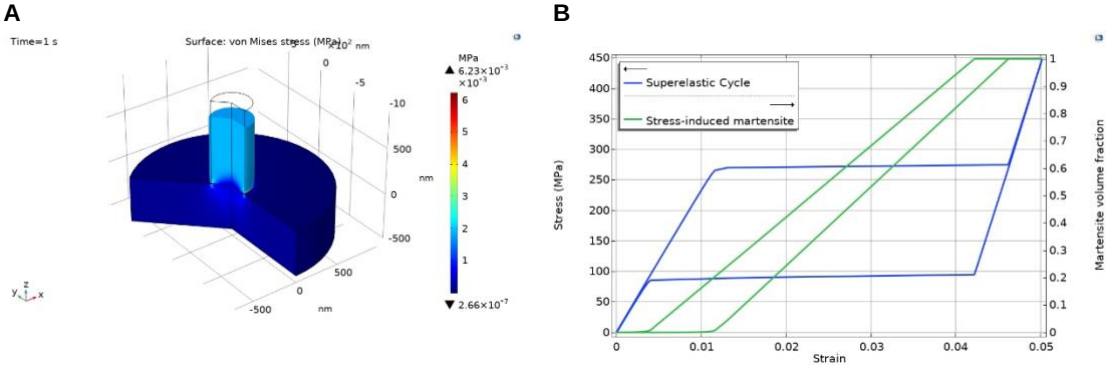

Figure 2: A) pillar with a diameter of 400 nm and a height of 900 nm. B) Scheme of a nano-compression test. C) Scanning electron image of a micropillar. D) Superelastic response of the pillar to a nano-compression test.

Conclusion

The newly developed model provides a unique opportunity to indirectly investigate the eCe, potentially paving the way for the creation of advanced cooling and heating nano-pumps for micro and nanoscale refrigeration.

References

1. X. Moya, S. Kar-Nayaran, N.D. Mathur, Caloric materials near ferroic phase transitions, *Nat. Mater.*, **13**, 439 (2014).

2. X. Moya, N.D. Mathur, Caloric materials for cooling and heating, *Science*, **370**, 797 (2020).

3. S. Quian, et al., High-performance multimode elastocaloric cooling system, *Science*, **380**, 722 (2023).

4. S. Quian, Y. Geng, et al., A review of elastocaloric cooling: materials, cycles and system integrations, *Int. J. Refrig*., **64**, 1 (2016).
5. J.F. Gómez-Cortés, et al., Size effect and scaling power-law for superelasticity in shape memory alloys at the nanoscale, *Nat. Nanotechnol*. **12**, 790 (2017).
6. J.F. Gómez-Cortés, et al., Ultrahigh superelastic damping at the nano-scale: a robust phenomenon to improve smart MEMS devices, *Acta Mater*. **166**, 346 (2019).

Iberian
COMSOL Multiphysics
CONFERENCE
Málaga. June 28, 2024

P1

Modelling and Simulation of a Fixed Bed Photocatalytic reactor: Influence of Some Design Variables on its Performance.

Carlos Macías[1,2]*, Alejandro Cifuentes-López[3]

[1] PROYMATICA 21 S.L.
[2] CM Biolab 2020 S.L.
[3] Addlink Software Científico, S.L.
*Corresponding author: carlosmacias@cmbiolab.com, carlosmacias@proymatica21.com

Introduction

Photooxidation processes (POP) have been subjected to intensive research since the last four decades and are currently used for water treatment. POPs can be performed in homogeneous phase, inducing the formation of active radical species by direct photolysis of dissolved peroxides, like H_2O_2 or in a heterogeneous phase, in which radicals are induced through a solid catalyst. Heterogeneous Photocatalytic oxidation (HPO) comprises a set of technologies in which a semi-conductor material like TiO_2, generates electron-hole pairs by photon excitation, being holes used for the generation of radical species [1], which in turn are responsible of organic contaminants degradation [2]. HPO technology can be classified in two groups: slurry-type reactors and fixed-bed reactors. In the first, the photocatalyst is dispersed as micro or nanoparticles in the water to be treated, being separated in a downstream unit and recycled back into the process. In the second, the catalyst is supported in a solid which can adopt different shapes and is immobilized in the reactor. The first type has the advantage of a larger surface per unit volume exposure but the drawback of needing a downstream process to recover the catalyst, usually expensive and difficult to manage. The fixed bed reactor avoids this drawback, but at the cost of a significant smaller surface exposure and higher head-loss, which could be critical, specially in gas phase reactors. Since the emitted light is rapidly absorbed in the fixed bed due to the shape and distribution of the solid supports, only a small fraction of the active material is used in the process giving place to low degradation rate-to-catalyst ratios. To increase this efficiency index, an HPO design is proposed in which the active material is cast onto the solid support in a thin layer of micron order thickness, which is exposed directly to light source. This configuration allows for a 100% exposure of the active material and can be applied either in flat surface or annular-type reactors allowing for different support geometric designs to increase the exposed surface to volume ratio (fig. 1). In the present work, a multyphysics model of organic contaminants HPO on TiO_2, based on the Tourchi-Ollis reaction mechanism [2-3] is proposed, supplying a theoretical framework and an engineering tool based on multyphysics modelling and simulation, which can be useful in providing insights into interrelations of unit performance with geometry, operational parameters and catalyst material, and in design optimization of HPO units.

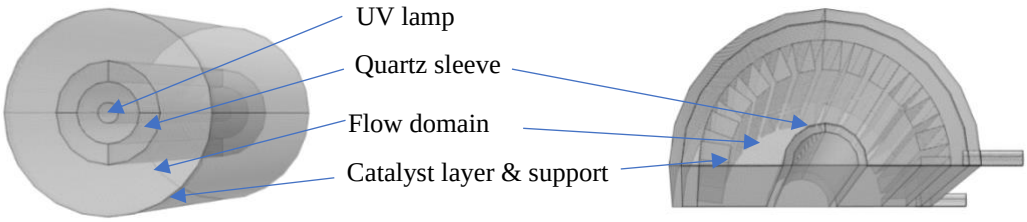

Figure 1: Photochemical reactor configuration. Simple axisymmetric plain geometry (left) and complex catalyst support geometry (right).

Use of COMSOL Multiphysics

For the present work five different COMSOL Multiphysics physics modules have been used. Figure 2 depicts the different physics used and their relationships.

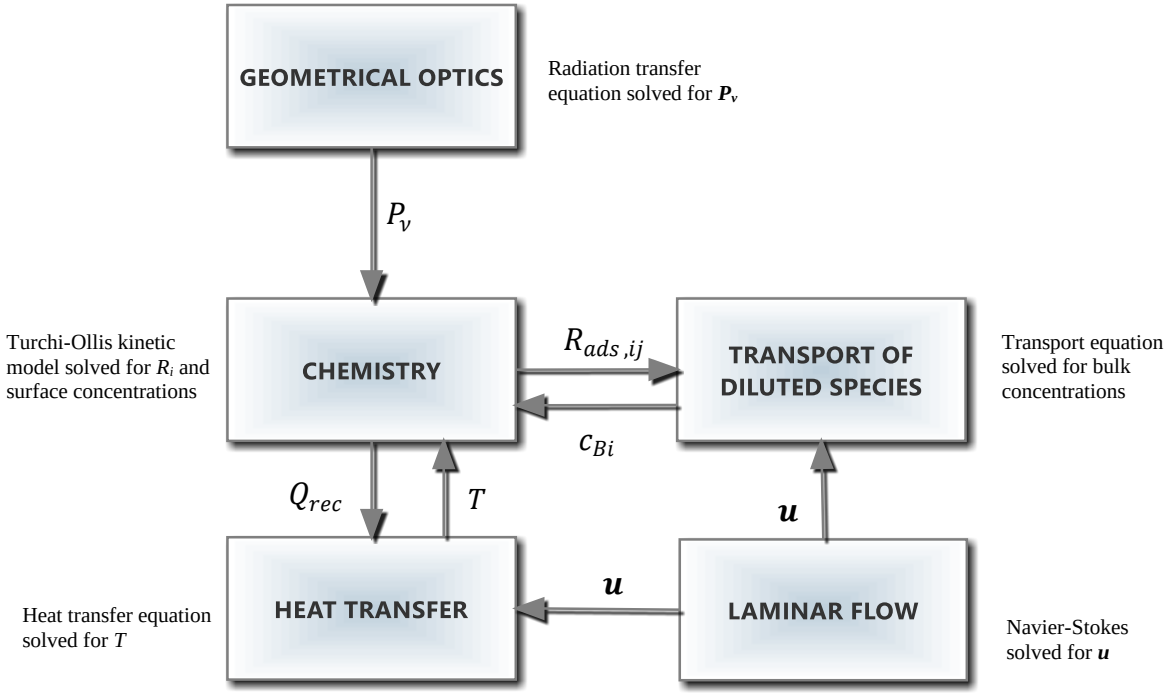

Figure 2: Physics modules interrelationships and contributions scheme

Results

The model in figures 1 and 2 has been run using experimental values for kinetic constants [3]. Results of phenol surface concentration profile and radiation fluence rate in the flat surface annular reactor are shown in figure 3.

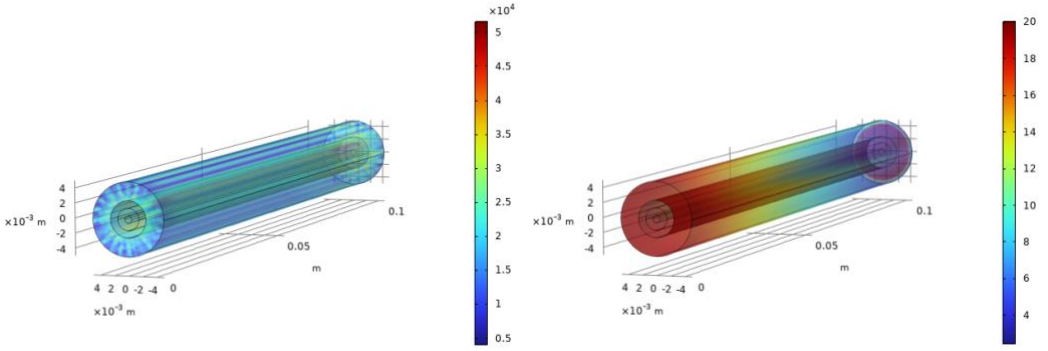

Figure 3: Radiation Fluence rate and phenol surface concentration in the annular flat bed photoreactor

Conclusion

The present study shows that multyphysics simulation is a useful tool for the analysis and rational design of HPO devices with complex underlying physic-chemical processes, being just a starting point to further development of a more powerful tool for the design and optimization of more efficient devices implying multiscale and multyphisics phenomena.

References

1. H. Paul Maruska and Amalk. Ghosh, Photocatalytic Decomposition of Water at Semiconductor Electrodes. *Solar Energy* **20**. pp./A3-.458 (1978).
2. Craig S. Turchi and David F. Ollis. Photocatalytic Degradation of Organic Water Contaminants: Mechanisms Involving Hydroxyl Radical Attack. *Journal of Catalysis* **122**, 178-192 (1990)
3. A.Tolosana-Moranchel, J.A. Casas, J. Carbajo, M. Faraldos, A. Bahamonde. *Applied Catalysis B: Environmental* **200** 164–173 (2017).

Iberian COMSOL Multiphysics CONFERENCE
Málaga. June 28, 2024

P2

Exploring Heterogeneous Graphite Electrodes: Parametric Sweeping and Stochastic Generation Techniques for Simulation and Analysis Using COMSOL Multiphysics

Álvaro Abucide-Armas[1,2,*], Oier Arcelus[2], Ander Sánchez-Chica[1], Javier Carrasco[2,3], and Ekaitz Zulueta[1]

[1]Departament of Automatic Control and System Engineering, University of the Basque Country UPV/EHU, C/Nieves Cano 12, 01006 Vitoria-Gasteiz, Spain,
[2]Center for Cooperative Research on Alternative Energies (CIC energiGUNE), Basque Research and Technology Alliance (BRTA), Alava Technology Park, Albert Einstein 48, 01510, Spain,
[3]Ikerbasque, Basque Foundation for Science, Plaza Euskadi 5, Bilbao 48009, Spain
*Corresponding author: aabucide@cicenergigune.com

Introduction

The growing availability of microscopy tomography techniques[1] and the in-silico structure generation models, such as manufacturing simulations[2], stochastic methods[3], and machine learning[4] enables explicitly describing the 3D geometry of electrodes. This study employs a COMSOL Multiphysics model capable of simulating stochastically generated 3D porous electrodes with an in-house algorithm and graphite as the active material (AM). The algorithm compares the generated electrode's particle size distribution (PSD) with the PSD of real graphite scanning electron microscopy (SEM) images. Then, the carbon binder domain (CBD) is added and the final volume ratios are compared with their reference input values. Finally, the electrode is meshed with the Python pygalmesh package and converted to MPHTXT format.

Use of COMSOL Multiphysics

A modified version of the heterogeneous NMC electrode template has been employed to obtain the discharge curves of electrodes with different features and structures. A Model Method has been developed to iterate through different electrodes. Each electrode is given an index parameter value to allow parametric sweeping between the different meshes. This approach can be used to parallelize the simulations of the analyzed electrodes.

Results

To test the COMSOL Multiphysics model, an electrode of size 75×75×85 μm^3 and a porosity of 48 % has been simulated at 0.1C, 1C, and 3C discharge rates with 5 meshes of variable precision. The discharge curves for every mesh are very similar (Figure 1). However, the visualization of variables such as the electric potential shows these differences in precision. Electrodes with different porosities were also simulated to study the impact of electrode composition on the specific capacity (Figure 2).

(a)

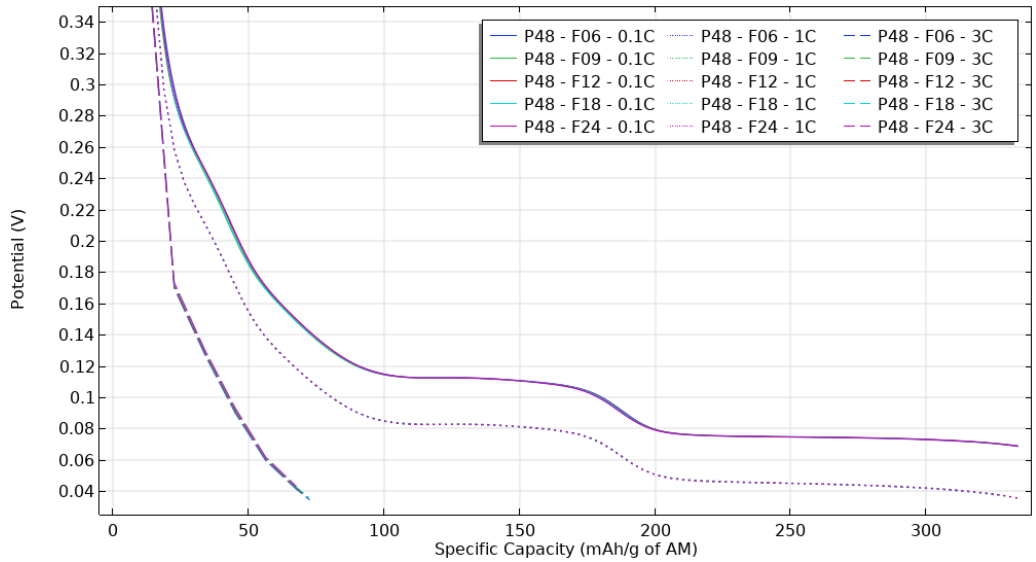

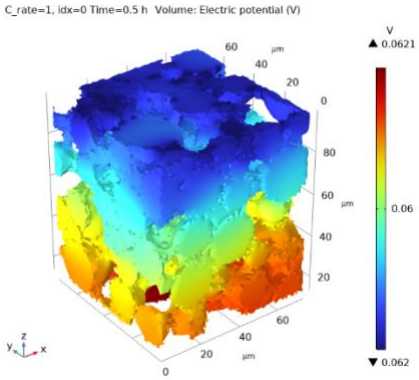

(b)

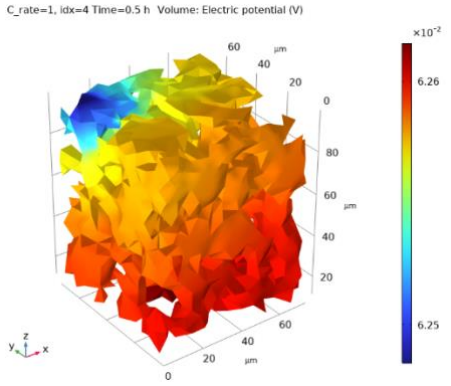

(c)

Figure 10: a) Discharge curves of a 48 % porosity electrode. b) Voltage field for F06 mesh precision (most precise). c) Voltage field for F24 mesh precision (least precise).

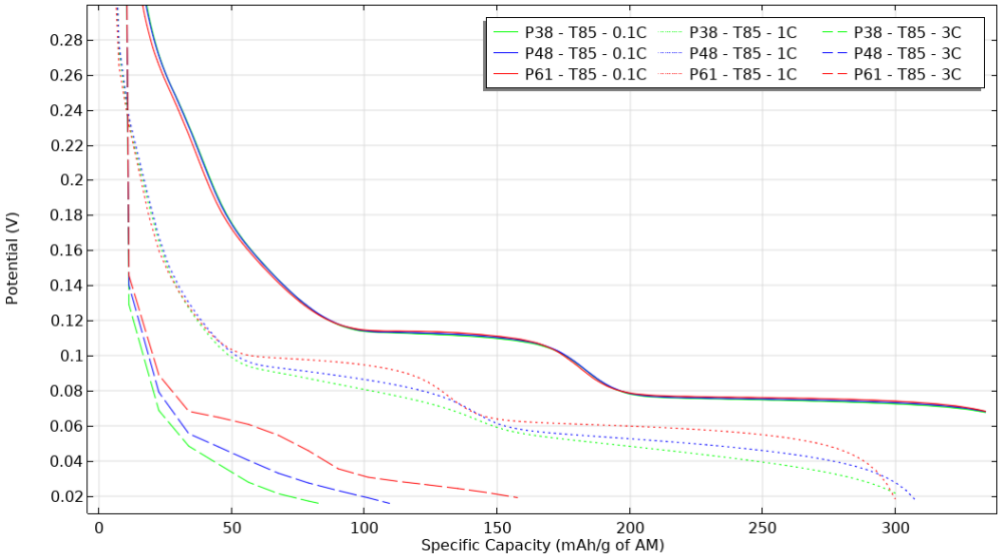

Figure 11: Simulated discharge curves for different porosities at 0.1C, 1C, and 3C.

Conclusion

This work presents a stochastic electrode generation algorithm able to create artificial structures with the desired properties. A mesh sweeping function has been developed to carry out parallelized simulations across different meshes. The presented COMSOL Multiphysics model is used to study LIB graphite electrodes' microstructure/performance relationships. Additionally, this algorithm can be adapted to structures with non-spherical particles (ellipses, realistic tomography-segmented particles, etc.) offering a flexible workflow to study electrode behavior under varying operating conditions.

References

1. Lu, X. *et al.* 3D microstructure design of lithium-ion battery electrodes assisted by X-ray nano-computed tomography and modelling. *Nat Commun* **11**, (2020).
2. Ngandjong, A. *et al.* Investigating electrode calendering and its impact on electrochemical performance by means of a new discrete element method model: Towards a digital twin of Li-Ion battery manufacturing. doi:10.1016/j.jpowsour.2020.229320ï.
3. Westhoff, D., Manke, I. & Schmidt, V. Generation of virtual lithium-ion battery electrode microstructures based on spatial stochastic modeling. *Comput Mater Sci* **151**, 53–64 (2018).
4. Kench, S. & Cooper, S. J. Generating 3D structures from a 2D slice with GAN-based dimensionality expansion. (2021).

Optimization of Energy Transmission through Waveguides, Antennas, and Dielectric Materials: An Integrated Approach to Wave Miniaturization

Alberto Frisa-Rubio[*1] y Carlos González-Niño[1]

[1]Área de Industria y Energía, CIRCE Centro Tecnológico
*Corresponding author: afrisa@fcirce.es

Introduction

The study of microwave energy transmission methods is critical for the advancement of efficient and versatile technologies. Waveguides, antennas, and dielectric-filled waveguides offer unique advantages in controlling and optimizing wave propagation. A key area of investigation is the modification of wave characteristics according to the transmission system employed.

This research delves into how the integration of dielectric materials within waveguides can modify wave dimensions, potentially leading to enhanced performance across various applications. Specifically, our study compares the performance and characteristics of different transmission systems—waveguides, antennas, and dielectric-filled waveguides—to achieve wave miniaturization while maintaining optimal performance.

By examining these systems, we aim to identify the most effective methods for reducing wave size without compromising efficiency, thereby contributing to the development of more compact and efficient technologies.

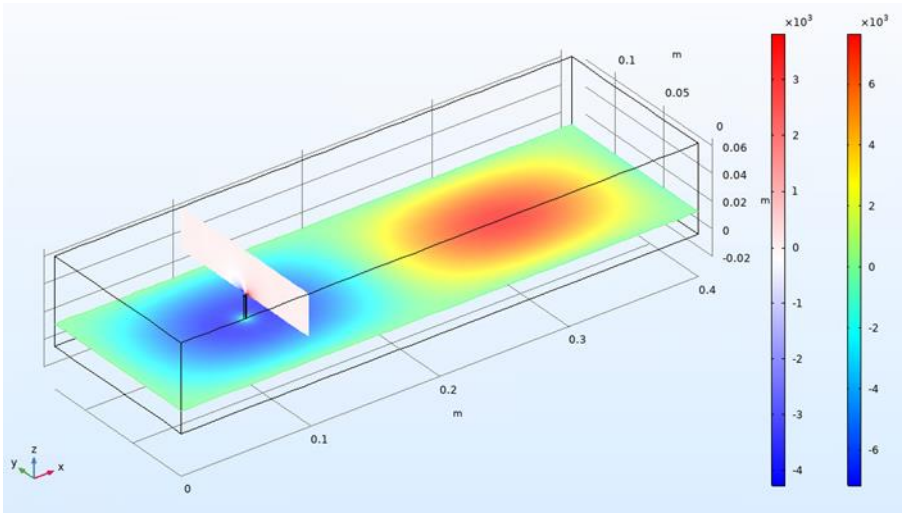

Figure 12: Waveguide transmission.

Use of COMSOL Multiphysics

The COMSOL Multiphysics software has been employed to model each transmission line [1], integrating the radiofrequency physics that characterizes the electromagnetic wave according to its frequency and power. By leveraging COMSOL Multiphysics' powerful simulation capabilities, we obtained the spatial distribution of the electric field throughout the volume in which it propagates. This detailed modeling allows for precise analysis and optimization of wave behavior within various transmission systems, emphasizing the software's robust handling of complex multiphysics interactions and its ability to provide high-resolution insights into electromagnetic field distributions.

Results

Different configurations of energy applicators were tested using a model implemented in COMSOL Multiphysics under consistent conditions of material, resonant cavity, and wave parameters. The results revealed varying performance levels from both energy efficiency and process effectiveness perspectives. These findings highlight the impact of applicator design on the overall transmission system's performance, demonstrating the importance of selecting the appropriate configuration for specific applications.

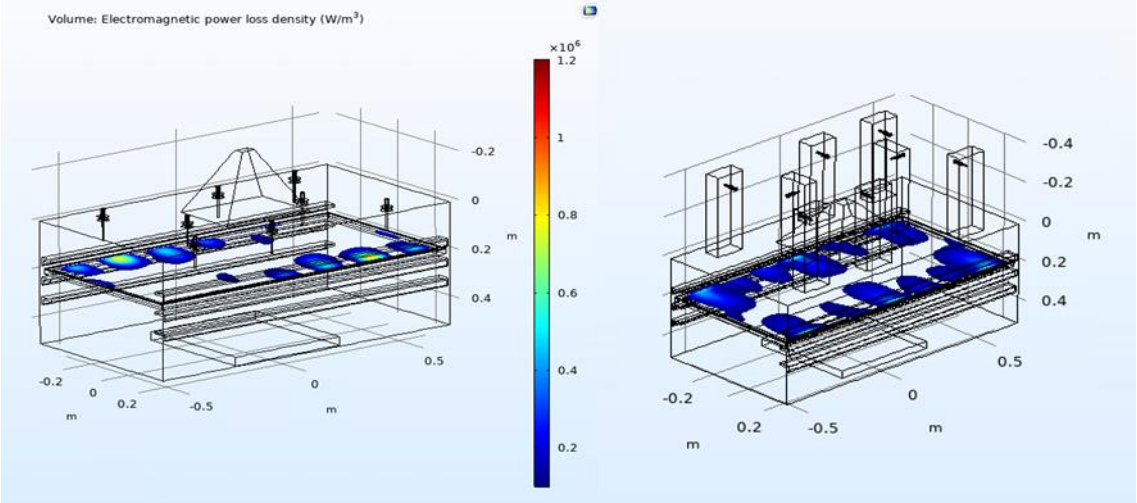

Figure 13: Reactor cavity study under the application since different transmission sources.

Conclusion

This study underscores the significant potential for innovation in the design and implementation of microwave energy transmission lines. By exploring various configurations and integrating dielectric materials within waveguides, we have demonstrated the ability to modify wave dimensions and optimize performance. The use of COMSOL Multiphysics has been instrumental in modeling and analyzing the complex interactions within these systems, providing valuable insights into the spatial distribution of the electric field.

The findings highlight the versatility and efficiency of different transmission line configurations, paving the way for the development of more flexible and adaptable microwave energy systems. These advancements can lead to improved efficiency, reduced system sizes, and enhanced applicability across a wide range of industries. Future research should continue to explore novel

materials and configurations to further enhance the performance and flexibility of microwave energy transmission technologies.

References

1. L. Zhao, X. Ming, G. Duan, Microwave heating of oil shale based on multiphysics field coupling: Positioning of the waveguide, International Journal of Heat and Mass Transfer, Volume 226, 125470 (2024).
2. Junling He, Yang Yang, Huacheng Zhu, Kang Li, Wei Yao, Kama Huang, Microwave heating based on two rotary waveguides to improve efficiency and uniformity by gradient descent method, Applied Thermal Engineering, Volume 178, 115594 (2020).

Acknowledges

This work has received funding by the European Union's Horizon Europe research and innovation programme under grant agreement No 101058540-PLASTICE project.

Funded by the European Union

Iberian COMSOL Multiphysics CONFERENCE
Málaga. June 28, 2024

P4

Dry Reforming of Biogas over Structured Catalysts: CFD Modelling and Simulation of Channels with Extreme Thermal Conditions

Felipe Costa[1*], Andrea Navarro-Puyuelo[1], Inés Reyero[1], Fernando Bimbela[1], Luis M. Gandía[1]

[1]Grupo de Reactores Químicos y Procesos para la Valorización de Recursos Renovables, Institute for Advanced Materials and Mathematics (InaMat[2]), Departamento de Ciencias, Edificio de los Acebos, Universidad Pública de Navarra, Campus de Arrosadía, E-31006, Pamplona, Spain.
* Corresponding author. Phone: +34948166298. E-mail: felipe.costa@unavarra.es

Introduction

Syngas production via catalytic dry reforming (DR) of methane is a highly endothermic chemical route for biogas valorization [1], usually accompanied by the reverse Water-Gas Shift (r-WGS) as side reaction. The use of structured catalytic reactors such as monoliths could be beneficial [2], owing to improved heat transfer and a superior reactor performance. Radial and axial thermal gradients can be important both at monolith and channel scales, though [3]. In this work, dry reforming of biogas was studied using a structured Rh catalyst deposited on monolithic channels, analyzing different operating conditions by CFD simulation and comparing them against experimental data.

Use of COMSOL Multiphysics

Coupled transport phenomena are modeled in 2D monolithic channels (RhM1/RhM4), with a porous domain symbolizing the catalytic zone. Meshing operations have been studied in order to achieve improved precision in contours and catalytic zones, with a work range of $98 – 751 \cdot 10^3$ elements. Parametric studies are performed on each channel geometry, for (1) catalytic layer thickness of 1-400 μm, (2) thermal boundary conditions in channel walls, (3) biogas inlet temperature between 600-800 °C, and (4) residence time of flow, with gas-hourly-space-velocity (GHSV) values among 45-7000 h^{-1}. Relevant variables of post-processing are species mass/molar fraction, CH_4 and CO_2 conversion, fluid temperature, reaction rates, and flow pressure and velocity.

Results

Figure 1 shows rates of generation and consumption for the main species taking part in DR and r-WGS reactions over the total channel length for isothermal and adiabatic simulations. While the DR reaction led to a linear diminution of the production rate for the involved species, the r-WGS reaction followed an asymptotic increase trend at the channel's first section ($L_c < 1/4$), after which the production rate remained quite stable, especially under adiabatic conditions (b). The prevalence of the DR at the selected conditions is responsible for the rapid CO_2 conversion once it is in contact with the catalytic layer at the channel inlet. As the fluid advanced along the channel, the CO_2 rate consumption by the DR reaction decreased and the r-WGS contribution increased.

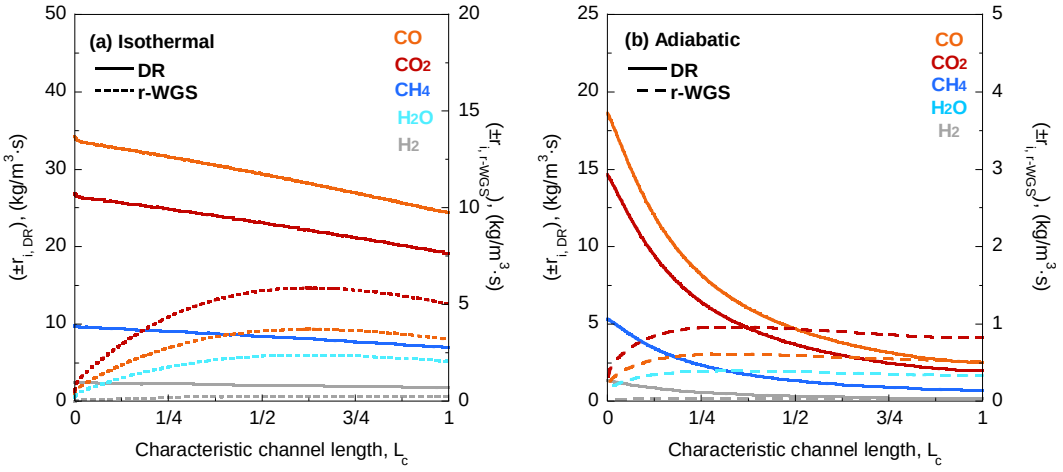

Figure 1: Evolution of production rates of CO_2, CH_4, CO and H_2 via DR and r-WGS reactions over the characteristic channel length (L_c), in the case of a RhM4 (δ = 70 µm) channel simulation, for (a) isothermal and (b) adiabatic operating conditions.

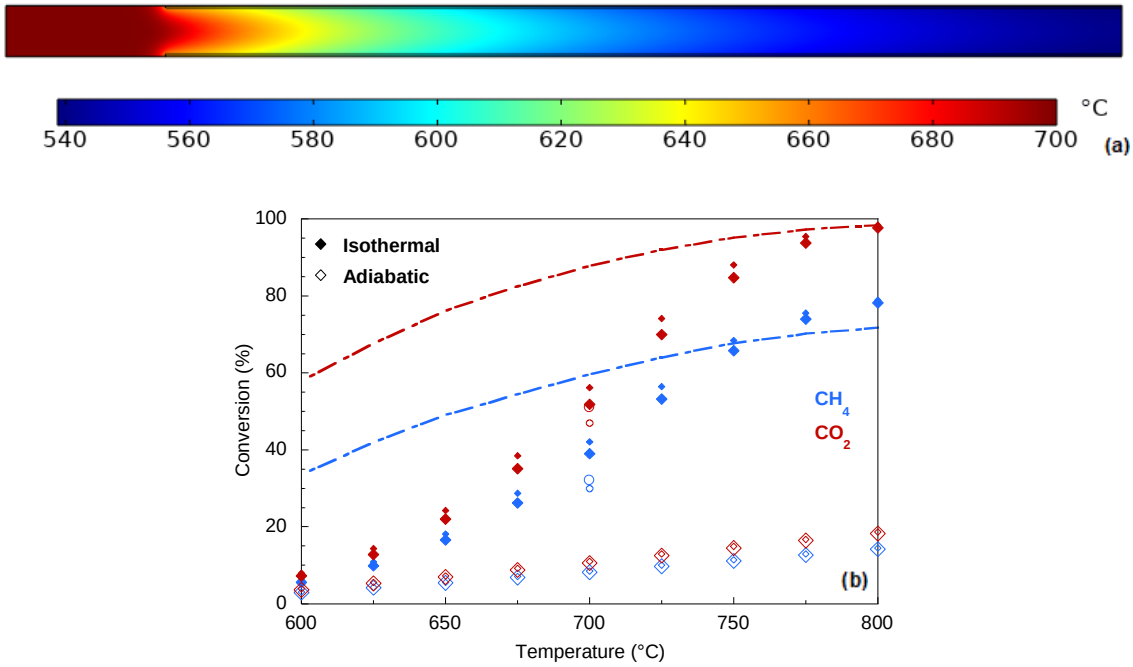

Figure 2: (a) Temperature profile along a RhM4 (δ = 70 µm) adiabatic channel simulation, and (b) influence of biogas temperature in CH_4 and CO_2 outlet final conversions for RhM1 (δ = 4 µm) and RhM4 (δ = 10 µm) channel simulations. Ovals (○) show experimental values. Lines describe the thermodynamic equilibrium data for CH_4 and CO_2 conversions.

Significant axial and radial temperature profiles for adiabatic cases are obtained, especially when L_c < 1/3, T_{inlet} > 700 °C, for the highest channel hydraulic diameter (RhM4), and for greater catalytic layer thicknesses (Figure 2a). Temperature decays of 160 and 45 °C were obtained, respectively. As for CH_4 and CO_2 outlet conversions (Figure 2b), comparison of empirical and CFD data evidenced that the lowest conversion values were achieved under adiabatic conditions, though showing some discrepancies; however, minimal differences were found using different

monolithic structures (RhM1/RhM4). In contrast, conversion values obtained in the isothermal simulations were closer to the experimental ones.

Conclusion

The performance of a Rh monolithic reactor in the dry reforming of biogas is highly affected by heat gradients, and important differences are found depending on the operation mode. Results obtained at a channel scale reveal that operation under isothermal conditions should be targeted, to minimize diffusional mass gradients through the catalytic layer and to ensure proper heat management at the reactor level.

References

1. D. Pakhare, J. Spivey. A review of dry (CO_2) reforming of methane over noble metal catalysts. *Chem. Soc. Rev.*, **43**, 7813-7837 (2014).
2. A. Navarro, Desarrollo de catalizadores basados en rodio y otros metales de transición para la producción de gas de síntesis a partir de biogás, thesis, Universidad Pública de Navarra (2021).
3. G. D. Wehinger, T. Eppinger, M. Kraume, Evaluating Catalytic Fixed-Bed Reactors for Dry Reforming of Methane with Detailed CFD, *Chem. Ing. Tech.*, **87** (6), 734-745 (2015).

Iberian COMSOL Multiphysics CONFERENCE
Málaga. June 28, 2024

P5

Numerical Simulation and Experimental Validation of a Micromachining Process on PDMS Membranes by Femtosecond Pulse Laser Ablation

Daniel Sánchez[*,1,2,3], Chahinez Berrah[2,3], Javier Rodríguez[2,3] y Andrés Sanz-García[1,2,3,4]

[1]Departament of Mechanical Engineering, University of Salamanca (Salamanca, Spain),
[2]Laser Applications and Photonics, University of Salamanca (Salamanca, Spain),
[3]Unit of Excellence in Structured Light and Matter, University of Salamanca (Salamanca, Spain),
[4]Institute of Biomedical Research of Salamanca, SACYL-University of Salamanca (Salamanca, Spain)
*Corresponding author: dasaga@usal.es

Introduction

Polydimethylsiloxane (PDMS) is a polymer widely used in many fields such as biomedicine and biology to build microfluidic devices called Organ-on-a-Chip (OoC) for cell culture [1]. Due to its excellent optical, mechanical, and chemical properties, the PDMS can be used to fabricate thin films that act as barriers in the OoCs. When replicating the human tissues, those PDMS membranes (thickness < 100 μm) should be of a controlled porosity by creating micro-holes of diameter and number proportional to the flow rate between those different compartments of OoCs (Figure 1).

Traditionally, soft lithography is the primary method for manufacturing the PDMS membranes. However, these techniques entail significant drawbacks such as high costs and rigid production. To provide more flexibility in their production, femtosecond laser ablation techniques could be an alternative to produce PDMS membranes with controlled porosity. Nevertheless, there are important roadblocks such as the lack of characterization studies in polymers, or the low number of studies simulating, and performing experimental procedures.

This study has been focused on validating a numerical simulation of femtosecond laser ablation by comparing it with experimental results obtained from different tests.

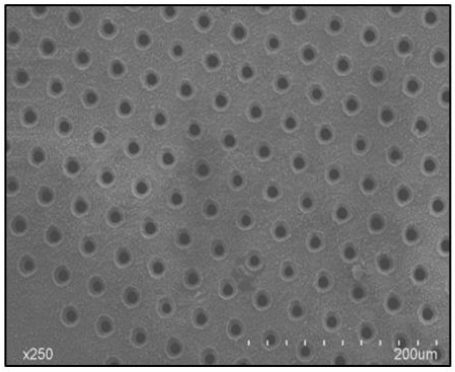

Figure 1. Matrix of micro-holes in a PDMS membrane.

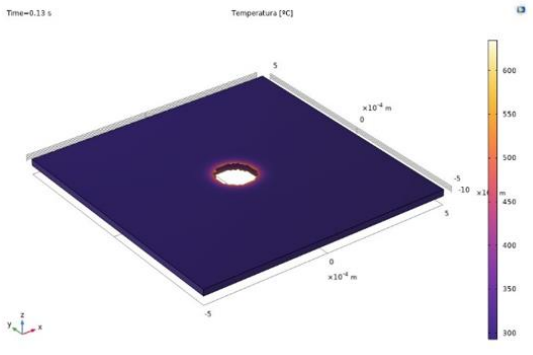

Figure 2. Simulation of the process in COMSOL Multiphysics 6.1.

Use of COMSOL Multiphysics

COMSOL Multiphysics is employed to model a numerical simulation of the technique (Figure 2). To recreate the process, the Heat Transfer and Solid Mechanics Modules are utilized.

The model is based on a 1 mm side and 100 µm thick square PDMS film, which is treated with a heat source that simulates a laser beam (Equations 1, 2, 3) [2]. The energy transferred by the laser is controlled by the activation time. The equations of energy used on the model are the classical expressions of heat transfer (Equation 4).

$$Q(x,y,z,t) = S(x,y,z) \cdot T(t) \tag{1}$$

$$S(x,y,z) = \frac{1 - R}{\delta + \delta_b} F \cdot \exp\left(- \frac{z}{\delta + \delta_b} - \frac{(x - x_0)^2 + (y - y_0)^2}{{w_0}^2} \right) \tag{2}$$

$$T(t) = \frac{1}{t_p} \sqrt{\frac{4 \ln 2}{\pi}} \exp\left(- 4 \ln 2 \left(\frac{t - 2t_p}{t_p} \right)^2 \right) \tag{3}$$

$$\rho C_p \frac{\partial T}{\partial t} + \rho C_p u \cdot \nabla T + \nabla \cdot q = Q \tag{4}$$

The material removal is established through a deactivation condition that mimics ablation, which is determined experimentally as a constant multiplied by the evaporation point of PDMS.

Results

The match between the experimental results, and those obtained from simulations is acceptable. The simulation allows for predicting the diameter and depth of micro-holes with satisfactory level of reliability based on the laser parameters.

Conclusion

The mathematical model developed can predict the output of micromachining processes based on a femtosecond laser ablation mechanism. This facilitates the adjusting of the parameters of the process without conducting any experimental tests.

References

1. F. Akther, et al., Surface Modification Techniques for Endothelial Cell Seeding in PDMS Microfluidic Devices, *Biosensors*, **vol. 10**, p. 182 (2020).
2. Li, Q., et al., Study of femtosecond ablation on aluminum film with 3D two-temperature model and experimental verifications, *Applied Physics A*, **vol. 105**, p. 125-129 (2011).

Iberian COMSOL Multiphysics CONFERENCE
Málaga. June 28, 2024

P6

Laser Spot Step Heating Thermography for Visualizing Heat Convection in a Fluid

A. Bedoya[1], J.B. Rojas-Trigos[1], J. Hernández-Wong*[2], A. Calderón[1], E. Marín[1]

[1]Instituto Politécnico Nacional, Centro de Investigación en Ciencia Aplicada y Tecnología Avanzada (CICATA), Unidad Legaria, Legaria 694, Colonia Irrigación, Delegación Miguel Hidalgo, Ciudad de México, 11500, México
[2]CONAHCYT- Instituto Politécnico Nacional, Centro de Investigación en Ciencia Aplicada y Tecnología Avanzada (CICATA), Unidad Legaria, Legaria 694, Colonia Irrigación, Delegación Miguel Hidalgo, Ciudad de Mexico, 11500, México.
*Corresponding author: hjoel@tetraa.com.mx, jhernandezwo@conahcyt.mx

Introduction

Visualizing a convective phenomenon is a novel application of laser spot step heating thermography [1]. A fluid confined in a measurement cell is in intimate contact with the inner face of a thin vertical metallic sheet, on whose external surface a laser beam is tightly focused, generating heat that diffuses to the closest part of the fluid layer adjacent to the sample, decreasing its density locally. This induces a density gradient that generates internal motion of the fluid, affecting thermograms recorded on the external side of the sheet, which is visualized after a given time has elapsed since the laser is switched on (Figure 1). The results of these measurements agree with those obtained using the finite-element analysis simulation software COMSOL Multiphysics®, and a simple model for free convection explains why the effect is only observed for some fluids.

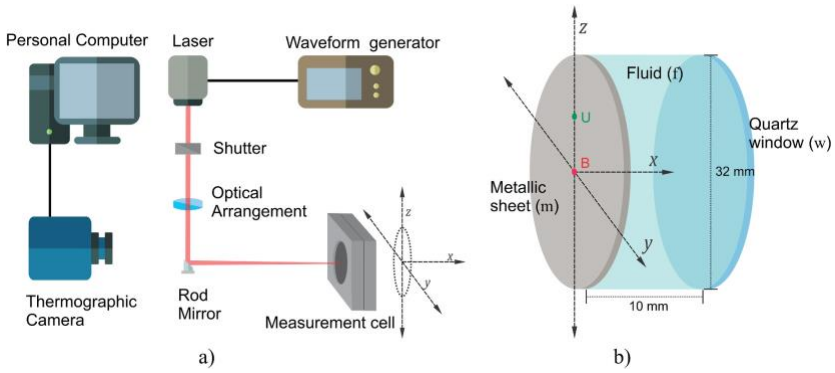

Figure 1. Schematic of the experimental setup (a) and the measurement cell (b)

Use of COMSOL Multiphysics

COMSOL Multiphysics is a powerful simulation software that allows engineers and scientists to model and simulate complex physical phenomena, such as those combining heat transfer and fluid flow processes. The measurement cell in Figure 1 was divided into four domains: the fluid (f), enclosed by the measurement cell, and the measurement cell subdivided into its components according to Figure. 1 b, which are the quartz window (w), the metallic sheet (m), and the container. The physical properties and the geometrical objects, including their limiting entities, were defined for each domain.

The physics modules employed in the simulation were the heat transfer in solids and fluids by the heat diffusion convection equation and mass and momentum transport for fluids by the Navier-

Stokes equation. A Tetrahedral conformal mesh was implemented to discretize the domain with 1,004,200 domain elements, and finally, a time steeping setting was configured in Strict mode [2] in the time-dependent solver.

Results

Figure 2 shows a good qualitative agreement in the shapes of the thermograms, with those corresponding to the experimental data observed. Figure 2 shows the radial profiles across the horizontal and vertical directions obtained from the experimental and simulated thermograms. The noise in the experimental points at larger distances from the excitation point is reduced as the excitation time increases the distance heat diffuses from the excitation point.

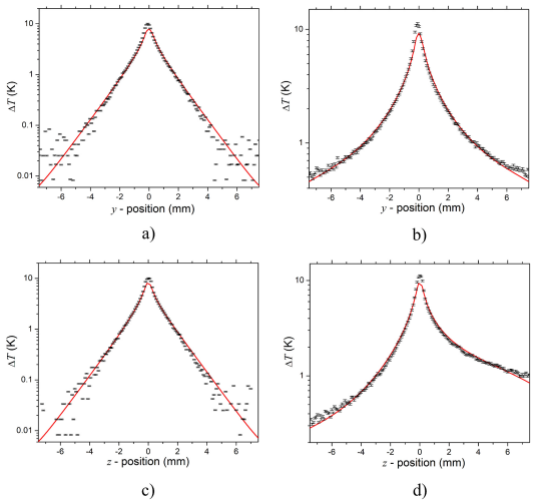

Figure 2: Comparison between experimental (black squares) and simulated (solid curves) temperature profiles in the sample. Across the *y*-axis: (a) 2 s, and (b) 120 s. Across the *z*-axis: (c) 2 s, and (d) 120 s.

Conclusion

Laser spot step heating active thermography for the visualization of a vertical laminar free convective flow in a liquid contained in a closed cell with a thin metallic wall subjected to punctual heating by continuous absorption of light energy is shown. Thermograms of the wall surface were acquired at different times after the beginning of excitation. These thermograms and temperature profiles along the vertical directions extracted from them show asymmetries reflecting the convection effects. Good agreement was found between experimental results and those of finite element computer simulations performed using COMSOL Multiphysics, which demonstrated that laser spot step heating thermography can be considered a simple, fast, and robust method for imaging laminar flows.

References

1. A. Salazar, M. Colom, A. Mendioroz, Laser-spot step-heating thermography to measure the thermal diffusivity of solids, Int. J. Therm. Sci. 170 (2021) 107124, https://doi.org/10.1016/j.ijthermalsci.2021.107124.

2. COMSOL Reference Manual. https://doc.comsol.com/5.5/doc/com.comsol.help.comsol/COMSOL_ReferenceManual.pdf. (Last Access on November 29, 2023).

Iberian COMSOL Multiphysics CONFERENCE
Málaga. June 28, 2024

P7

Computational-Aided Design of Continuous-Flow Systems for the Magnetic Recovery of Microplastics from Water

Cristina González-Fernández[1*], Eugenio Bringas[1], María J. Rivero[1], Inmaculada Ortiz[1]

[1]Departamento de Ingenierías Química y Biomolecular, Universidad de Cantabria, Avda. Los Castros, s/n, 39005, Santander (Spain)
*Corresponding author: gonzalezferc@unican.es

Introduction

Microplastics (MPs) have emerged as a major environmental concern in recent years due to the negative impact they pose on public health and ecosystems.[1] Hence, there exists an urgent need to develop efficient strategies for the successful removal of MPs from water resources. Magnetophoretic separation of MPs has garnered particular interest due to the proven potential of this method for extracting other contaminants (e.g., arsenic) from complex matrices.[2] Specifically, the magnetophoretic recovery of MPs relies on the magnetization of MPs by attaching magnetic nanoparticles to these entities; once the MPs are magnetized, the resulting magnetic MPs are retrieved by applying an external magnetic field. In this work, we move forward on the design of continuous-flow systems for the magnetophoretic extraction of MPs from water bodies.

Use of COMSOL Multiphysics

Herein, the COMSOL Multiphysics 6.2 software is used to model and simulate the two stages of the continuous-flow magnetophoretic system (CFMS) previously described. The CFMS considered in this study (Figure 1) consists of a channel with a Y-shaped inlet and outlet, where two regions can be easily distinguished, namely, the MPs sequestration and the magnetic separation stages. In the MPs sequestration stage, the magnetic nanoparticles are attached to the MPs when both streams are in contact. Then, the resulting MPs-bead complexes are collected through the outlet closest to the magnet, whereas a MPs and beads- free solution is obtained through the lower outlet. The magnetic force was provided by a NdFeB permanent magnet.
For modeling the magnetophoretic retrieval of MPs, several COMSOL Multiphysics modules were coupled. The “particle tracing for fluid flow” was used to predict the motion of the magnetic nanoparticles, MPs and the MPs-bead complexes in the CFMS. Moreover, the “laminar flow” interface within the “CFD” module was selected to account for the system fluid dynamics. Lastly, the “magnetic fields, no currents” physics of the “AC/DC” module was selected to model the magnetic field strength. COMSOL Multiphysics simulations were conducted on a 48-core workstation with 128 GB of RAM.

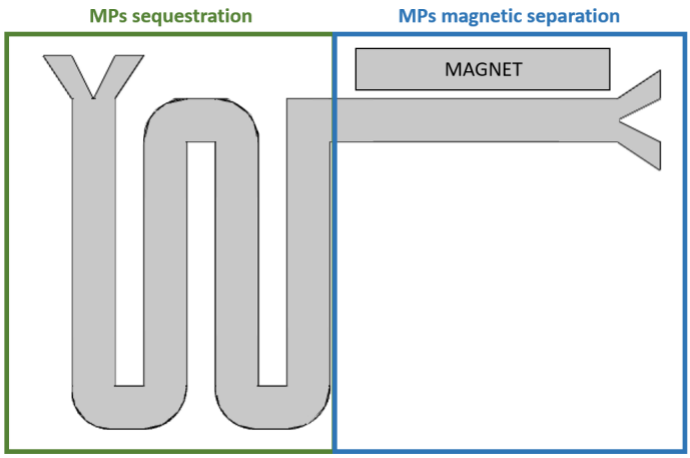

Figure 1: Schematics of the CFMS under investigation.

Results

Our initial findings suggest that complete magnetic recovery can be accomplished by introducing the MPs and magnetic nanoparticles at a velocity of 0.01 $m \cdot s^{-1}$. This result reveals that the CFMS under investigation enables processing relatively high flow rates and simultaneously ensuring the total retrieval of MPs. However, further simulations are required to identify the optimal operation conditions for the system, including the magnet dimension and position, or the ratio of concentrations between MPs and beads that should be introduced in the system.

Conclusion

The software COMSOL Multiphysics offers significant opportunities for the simulation of molecule capture coupled with magnetophoresis. Additionally, the methodology employed in this study can guide the computational-aided design of CFMS that could be applied for recovering a wide variety target entities beyond MPs.

Acknowledgments

Financial support from the project PID2021-122563OB-I00 funded by MICIU/AEI/10.13039/501100011033 and by "ERDF/EU", and grant PLEC2021-007718 funded by MICIU/AEI/ 10.13039/501100011033 and by the European Union NextGenerationEU/PRTR is gratefully acknowledged. Cristina González-Fernández also thanks the Spanish Ministry of Universities for the Margarita Salas postdoctoral fellowship (grants for the requalification of the Spanish university system for 2021-2023, University of Cantabria), funded by the European Union-NextGenerationEU.

References

1. Ali et al., Insight into microplastics in the aquatic ecosystem: Properties, sources, threats and mitigation strategies, *Science of the Total Environment*, **913**, 169489 (2024).
2. Saiz et al. Functionalized magnetic nanoparticles as new adsorption materials for arsenic removal from polluted waters, *Journal of Chemical Technology and Biotechnology*, **89**, 909-918 (2014).

Application of COMSOL Multiphysics in Electrical Infrastructure Simulation for Newly Graduated Engineers

Safaa El Ouariachi El Ouariachi[1*]

[1]Escuela de Ingenierías Industriales, University of Málaga
*Corresponding author: safaelouariachi@uma.es

Introduction

In electrical engineering, simulating the physical phenomena affecting infrastructures is crucial but not always perceptible or visually clear. As a recent graduate in industrial design engineering and starting out in the electrical field, I have observed that advanced simulation programs like COMSOL Multiphysics could be essential for technicians. These programs allow for detailed analysis of aspects such as voltage drop and cable saturation based on their section and material. (Figure 1).

Use of COMSOL Multiphysics

Working with electrical lines and investigating their behavior under various conditions requires deep analysis that often goes beyond simple calculations. As we explore everything from transformation centers to high-voltage substations, we face a series of complex phenomena. These challenges motivate me to use COMSOL Multiphysics to better visualize and understand these processes and, in turn, share this knowledge with other newcomers in the field.

Results

My goal is to effectively use COMSOL Multiphysics to model electrical phenomena and improve training for new engineers in understanding and managing our electrical infrastructures. This approach will not only facilitate my professional development but will also enhance the teaching and learning capacity within my work environment.

Conclusion

The use of COMSOL Multiphysics in the context of electrical engineering offers a powerful tool for visualizing and analyzing phenomena that would otherwise be abstract or difficult to understand. This conference represents an ideal opportunity to explore how advanced simulation can transform our approach to electrical infrastructures, benefiting both experienced professionals and those starting their careers.

References

1. Lee, M. & Kim, J., "Advanced Applications of COMSOL Multiphysics in Electrical Engineering Studies", *Journal of Applied Simulation*, **15**(3), 134-145 (2021).
2. Patel, R., Thompson, S., "Integrating Machine Learning with Multiphysics Models for Smart Grid Analysis", *International Journal of Electrical Power Systems*, **22**(2), 88-97 (2022).
3. Johnson, L. & Gupta, N., "Simulation-Based Optimization of High Voltage Transmission Lines", *Electrical Engineering Insights*, **18**(1), 201-210 (2020).

4. Brown, F., "Utilizing COMSOL Multiphysics for Enhanced Understanding of Electromagnetic Fields in Substations", *Journal of Modern Power Systems*, **29**(4), 422-430 (2023).
5. Zhang, Y., "The Role of Simulation Tools in Undergraduate Electrical Engineering Education", *Journal of Engineering Education*, **12**(1), 37-45 (2019).

Design and Proof of Concept of Micro-Dampers based on Nano-Pillars of Shape Memory Alloys to Improve MEMS Reliability

Jose M. San Juan[*1], Jose F. Gómez-Cortés[1], Emilio Ruiz[2], Eduardo González[3] y Maria L. Nó[1]

[1]Department of Physics, University of the Basque Country (Spain),
[2]Department of Applied Physics II, University of Málaga (Spain),
[3]COMSOL AB (Sweden).
*Corresponding author: jose.sanjuan@ehu.es

Introduction

Shape Memory Alloys (SMA) are smart functional materials exhibiting the properties of shape memory and superelasticity due to a reversible thermoelastic martensitic transformation (MT) [1, 2]. SMA are also considered as High-Damping Materials (HDM) due to the dissipation of mechanical energy associated with the reversible motion of the martensite interfaces. This property could become particularly useful at small scale to damp noisy vibrations in Micro-Electromechanical Systems (MEMS), improving their service life and reliability. Indeed, an ultra-high mechanical damping was reported in nano pillars of Cu-Al-Ni SMA [3] fabricated by focused ion beam (FIB) technique, and further studies confirmed the robustness of this damping behavior on cycling and time [4]. In addition, a noticeable size-effect on the critical stress to induce the MT during the superelastic behavior was reported at micro/nano scale [5]. These previous results anticipate the possibility of developing micro-dampers based on arrays of nano pillars, that stacked with a gradient of pillar diameters could offer extremely high mechanical damping in confined volumes. The present work is a first approach to use the computing capabilities of COMSOL Multiphysics to generate not only the design of the stacks of arrays of micro/nano pillars, but also to make a proof of concept, simulating the dissipated energy per unit of volume.

Use of COMSOL Multiphysics

COMSOL Multiphysics was employed to simulate the strongly non-linear behavior of Cu-Al-Ni SMA during the superelastic effect, using the Souza-Auricchio model, already implemented in the COMSOL Multiphysics module of Non-linear Structural Mechanics. Then, the first step was to create a “new group of materials” in the users material library, because such kind of SMA was not yet included. The second step was to develop a model of Pillar as realistic as possible, this means similar to the ones milled by FIB, which exhibits rounded edges and a typical milling taper. This was done using an axisymmetric geometry to minimize computing cost. Finally, a first series of arrays of pillars with different diameters were constructed and computationally tested.

Results

To understand the results, let us introduce the target of the simulations. In Figure 1a, a real FIB milled pillar of about 1μm mean diameter is presented, and Figure 1b shows its superelastic response at nanoscale from reference [5]. Then, in Figure 1C the COMSOL Multiphysics generated pillar with rounded filets and 2º taper is shown over a base (representing the bulk remaining material), in which the cylindrical external surface was restricted in X-Y displacement.

The displacement along the Z-axis, for both Pillar and base, is indicated in the lateral bar for the maximum strain. To simulate the stress-strain curve of Figure 1d, the size effects on the critical stress were not yet taken into account, and consequently the level of stresses in the experimental and simulated curves are not equivalent. Nevertheless, the qualitative agreement is noticeable, particularly the apparition of several domains in the slope of hardening in the superelastic plateau. The next step was to create arrays of pillars similar to the ones obtained by FIB milling. An example of such arrays is shown in Figure 2a, and in Figure 2b the geometrically generated array to be tested. In our complete work, several arrays of pillars with different diameters are built and tested.

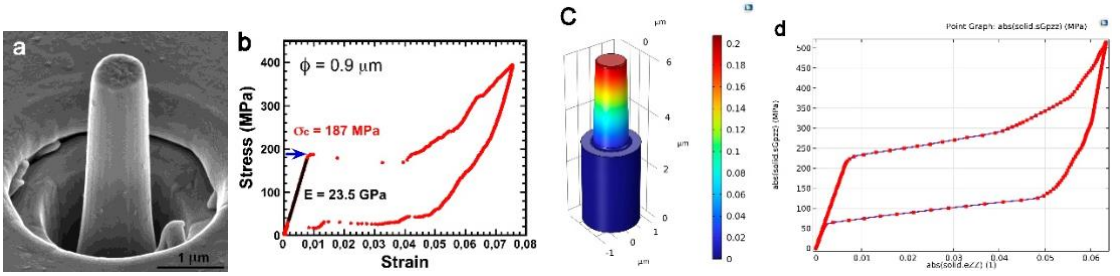

Figure 1: (a) Pillar milled by FIB and (b) it s superelastic Cycle (from [5]). (c) Generated pillar with 2º taper on its bulk base; the displacement, at the maximum load of 500 MPa, is indicated by the color scale. (d) Superelastic nano-compression cycle simulated in the pillar from (c).

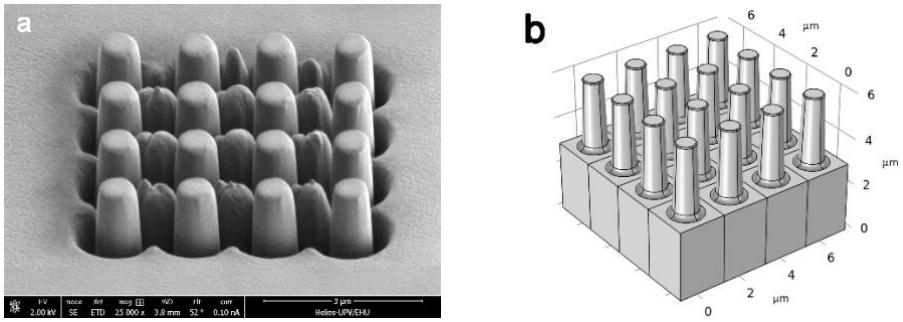

Figure 2: (a) Scanning electron microscopy of the array milled by FIB. (b) Array of pillars generated from the pillar shown in Figure 1c. Both, experimental and simulated are ready to be tested.

Conclusion

The Non-linear Structural Mechanics module from COMSOL Multiphysics, offers very good capabilities to simulate the real behavior of the SMA at nanoscale. These results pave the way for the design and proof of concept of many potential devices to be used in MEMS technology.

References

1. K. Otsuka, C.M. Wayman (Eds.), *Shape memory Materials*, Cambridge Univ. Press, UK (1998).
2. K. Yamauchi, I. Ohkata, K. Tsuchiya, S. Miyazaki (Eds.), Shape Memory and Superelastic Alloys, Oxford-Woodhead Publishing, Oxford, UK (2011).
3. J. san Juan, M.L. Nó, C.A. Schuh, Nanoscale shape-memory alloys for ultrahigh mechanical damping, *Nature nanotechnology*, **4**, 415-419 (2009).

4. J.F. Gómez-Cortés, M.L. Nó, I. Ruiz-Larrea, T. Breczewski, A. López-Echarri, C.A. Schuh, J.M. San Juan, Ultrahigh superelastic damping at the nanoscale: A robust phenomenon to improve smart MEMS devices, *Acta Materialia*, **166**, 346-356 (2019).
5. J.F. Gómez-Cortés, M.L. Nó, I. López-Ferreño, J. Hernández-Saz, S.I. Molina, A. Chuvilin, J.M. San Juan, Size effect and scaling power-law for superelasticity in shape-memory alloys at the nanoscale, *Nature nanotechnology*, **12**, 790-796 (2017).

Iberian COMSOL Multiphysics CONFERENCE
Málaga. June 28, 2024

P10

Using COMSOL Multiphysics to Simulate the Superelastic Behavior in Shape Memory Alloys for Aerospace Applications

Ander Abadín*[1], José F. Gómez-Cortés[1], María L. Nó[1] y José M. San Juan[1]

[1]Department of Physics, University of the Basque Country (Spain).
*Corresponding author: aabadin001@ikasle.ehu.eus

Introduction

Shape memory alloys (SMA) are considered as smart materials because of their functional properties of superelasticity and shape memory, which are finding many applications in practically all the industrial sectors, exhibiting a particularly high-added value in the aerospace and bio-medical sectors [1]. The physics behind the shape memory and superelasticity is a reversible martensitic transformation associated with an atomic shearing of the crystalline lattices, exhibiting a strong non-linear behavior and a critical dependence on temperature around the phase transition temperatures. However, these properties make difficult the design of components and devices, because during the service working conditions they will operate in a three-dimensional space stress-strain-temperature. In addition, the main SMA, like Ni-Ti or Cu-Al-Ni, could exhibit and anisotropic behavior that must be taken into account in the design of specific devices. Then, the present work is a first approach to the analysis of the thermo-mechanical behavior of two SMA, the Ni-Ti and the Cu-Al-Ni, with view to further applications in the bio-medical and aerospace sectors. This analysis is approached through the simulation by COMSOL Multiphysics, and the comparison of the computed solutions with the results experimentally measured on specific SMA developed for space applications [2].

Use of COMSOL Multiphysics

The COMSOL Multiphysics software was employed to simulate the non-linear behavior of SMA. Initially, the two different models for simulation of SMA behavior, which are already included in the "Non-linear Structural Mechanics" package of COMSOL Multiphysics, have been tested in order to compare their capabilities and friendliness. Then, several parameters have been optimized in to get a good match between the computed solutions and the real behavior of the SMA. Further multiphysics capabilities will be explored in the next future to optimize the use of this software for the prediction of the response of SMA devices.

Results

Special care has been taken in the meshing to adapt to the geometry in the simplest way, without losing accuracy. The simulation has been carried out under axisymmetric regime, and in Figure 1 the initial meshing and the stresses distribution is indicated under maximum load and when the load is withdrawn. Moreover, the influence of the studied point has been analyzed with the aim of visualizing how the superelastic behavior vary depending on the geometry. The superelastic cycling at different maximum strains, presented in Figure 2, qualitatively agree with the expected behavior. In the complete work, the superelastic behavior is computed for different kind of SMA and compared with its real experimental behavior.

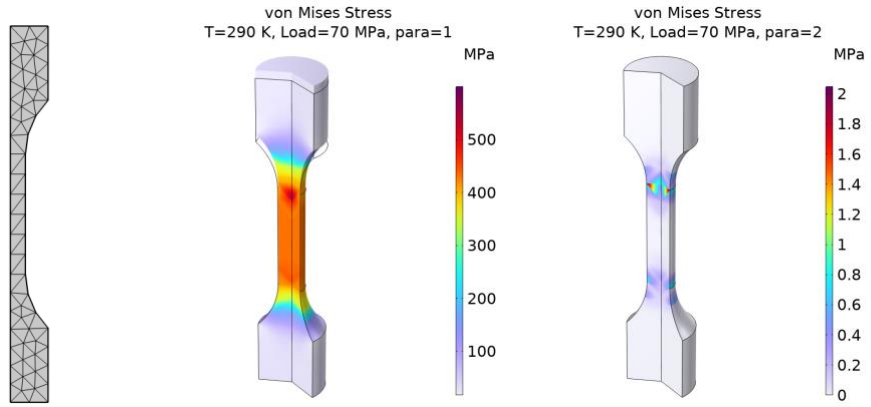

(a) (b) (c)

Figure 1: (a) Meshing of the bone-shaped study sample. (b) and (c) von Mises stress for the NiTi alloy in the Lagouda's model when the load is maximum (b) and after unloading (c).

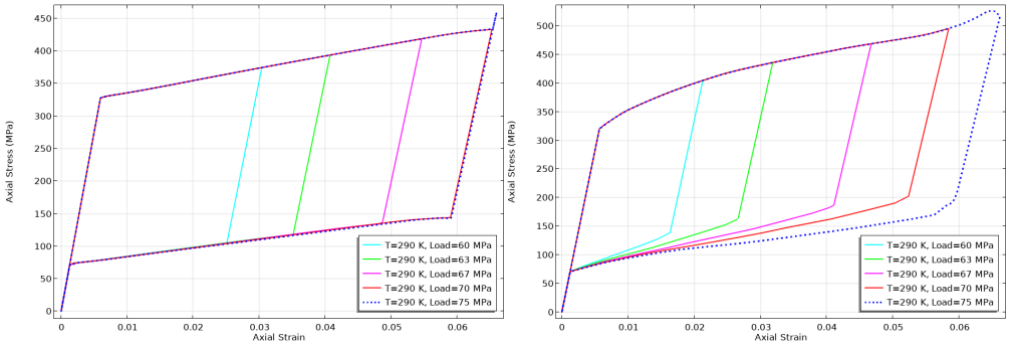

(a) (b)

Figure 2: Superleastic effect for the NiTi alloy in the Lagouda's model at 290 K in (a) the center of the sample and (b) the point of intersection between the curve and the line (in the constriction).

Conclusion

This work shows the capabilities of simulating the real tensile test of shape memory alloys in their superelastic region using COMSOL Multiphysics. Through the comparison, we can identify both similarities and areas for improvement. Ultimately, we aim to leverage these findings to develop models of real objects such as micro-electro-mechanical systems (MEMS) using this software.

References

1. J.M. Jani, M. Leary, A. Subic, M.A. Gibson, A review of shape memory alloy research, applications and opportunities, *Matter & Design*, **56**, 1078-113 (2014).
2. I. López-Ferreño, J. Gómez-Cortés, T. Breczewski, I. Ruiz-Larrea, M.L. Nó, J.M. San Juan, High-temperature shape memory alloys based on the Cu-Al-Ni system: design and thermomechanical characterization, J. Matter. Res. & Tech., **9**, 9972-9984 (2020).

Iberian COMSOL Multiphysics CONFERENCE
Málaga. June 28, 2024

P11

Analyzing Total Hip Arthroplasty: Straight Stem vs Anatomical Stem with Different Materials and Activities

Pedro Queirós[2], Nuno Gueiral[1,2*], Carlos David González-Gómez[3,4]

[1] Physics Department, Porto Superior Engineering Institute (ISEP), Portugal
[2] Center for Innovation in Engineering and Industrial Technology, Porto Superior Engineering Institute (ISEP), Portugal
[3] Department of Applied Physics II, Universidad de Málaga, 29071, Málaga Spain
[4] Nanoparticles Trapping Laboratory, Department of Applied Physics, Universidad de Granada, 18071, Granada, Spain
*Corresponding author: ndg@isep.ipp.pt

Introduction

Total Hip Arthroplasty involves replacing damaged parts of the hip joint with a prosthetic comprised of an artificial acetabular cup and femoral head. These components, made of durable, low-friction materials, aim to restore mobility, and alleviate pain in patients with hip joint degeneration, such as osteoarthritis or fractures. Utilizing computational mathematical models, such as the finite element method (FEM), it is possible to predict the behavior of materials under simulated loads from common daily activities [1], thereby anticipating potential failures in the femoral stem or the material itself.

Use of COMSOL Multiphysics

In this investigation, we address the performance analysis of two prostheses: cemented and cementless, exploring the influence of stem design using numerical simulation with COMSOL Multiphysics software. Through data analysis from a Portuguese hospital and *OrthoLoad database* [3]., the two stems analyzed were the *Exeter* (cemented) [2,3,4] and the *Accolade* (cementless) [5], both from the *Stryker*. The bone material considered was cancellous bone, with implant materials being Cobalt-Chromium (Co-Cr) and Titanium (Ti-6Al-4V). Under the conditions, it was necessary to generate a highly refined computational mesh with a very small size element for contact boundaries between the two surfaces, particularly around the implant, to ensure a high-resolution quality in these areas. For the Exeter stem, a thin layer of Poly(methyl methacrylate) (PMMA) was added to simulate the cement used in cemented prostheses. This PMMA layer represents the thermal properties of the cement, defining the resistive material on boundaries.

Results

This numerical analysis was conducted in a stationary manner, meaning there was no temporal variation. It focused solely on determining stress distribution and displacements during activities such as walking, ascending stairs, descending stairs, standing up, sitting down, stand on one leg, and kneeling, while applying maximum load to the femoral head. The static analysis showed that ascending and descending stairs resulted the highest stress peaks on the implant, regardless of the material used, suggesting these activities impose significantly greater loads on the hip joint compared to other activities. The maximum displacement occurred at the femoral head for both

material variants across all activities, with very similar values, indicating that the femoral head area is critical for movement during all activities, irrespective of stem material. For all activities evaluated, the *Accolade* exhibited significantly higher stress values than the *Exeter*, which may indicate that the *Accolade* stem absorbs less load, potentially leading to greater bone wear over time.

Conclusion

This study aimed to evaluate the performance of Stryker hip stems, specifically the *Exeter* and *Accolade* models, comparing the materials Cobalt-Chromium and Titanium. Comprehensive tests were conducted to simulate various daily activities encountered by patients undergoing Total Hip Arthroplasty. The analysis focused on identifying the maximum stress points during these activities to understand the areas where the stem structure is most challenged, as well as the maximum displacement points to assess load absorption capacity and stem behavior under pressure.

References

1. M. O. Heller, G. Bergmann, J. P. Kassi, L. Claes, N. P. Haas, and G. N. Duda, "Determination of muscle loading at the hip joint for use in pre-clinical testing," *J Biomech*, **38**(5), pp. 1155–1163, May 2005, doi: 10.1016/j.jbiomech.2004.05.022.

2. H. D. W. Williams, G. Browne, G. A. Gie, R. S. M. Ling, A. J. Timperley, and N. A. Wendover, "The Exeter universal cemented femoral component at 8 to 12 years. A study of the first 325 hips," *J Bone Joint Surg Br*, **84** (3), pp. 324–334, 2002, doi: 10.1302/0301-620X.84B3.12261.

3. https://orthoload.com/database/?implantid

4. Clemente, N. D., Yapp, L. Z., Baxendale-Smith, L. D., MacDonald, D., Howie, C. R., & Gastão, P. (2023). Exeter® cemented with standard stem versus short stem when used for primary total hip arthroplasty: A survival analysis. Arthroplasty, 5(Article 47). https://doi.org/10.1186/s42836-023-00200-8

5. Wyatt, M. C., Poutawera, V., Kieser, D. C., Frampton, C. M. A., & Hooper, G. J. (2020). How do cemented short Exeter stems perform compared with standard-length Exeter stems? The experience of the New Zealand National Joint Registry. Arthroplasty Today. https://doi.org/10.1016/j.artd.2020.01.003

5. Ueoka, K., Kabata, T., Kajino, Y., Inoue, D., Ohmori, T., Yamamuro, Y., Tsuchiya, H. (2023). Five-year clinical and radiographic outcomes of Accolade TMZF and Accolade II stem use. Journal of Joint Disorders and Orthopedic Surgery Research. https://doi.org/10.1016/j.jjoisr.2023.09.004

Iberian COMSOL Multiphysics CONFERENCE
Málaga. June 28, 2024

P12

THCM Modelling of Nuclear High-Level Waste cells

Miquel de la Iglesia*[1], Marcelo Laviña[1], Joan Pelegrí[1], Emilie Coene[1], Arnau Pont[1], Andrés Idiart[1], Benoit Cochepin[2]

[1]AMPHOS 21 Consulting S.L., Carrer de Veneçuela, 103, 08019 Barcelona, Spain.
[2]Andra, Scientific & Technical Division, 1-7 Rue Jean Monnet, Châtenay-Malabry F-92298, France
*Corresponding author: miquel.iglesia@amphos21.com

Introduction

Prior to establishing a deep geological repository for radioactive waste in claystone, understanding the long-term performance of the engineered barriers surrounding the high-level waste is crucial. In this framework, a 2D-axisymmetric one-way-coupled thermo-hydro-chemo-mechanical (THCM) modelling study of a high-level waste (HLW) cell of the Cigéo project in France is presented. HLW cells are composed of several engineered components and natural barriers including a bentonite-based plug, steel liners and overpacks, cementitious grout, clay-based backfill material, concrete structures, and the Callovo-Oxfordian claystone (Figure 1). The THCM model analyses system performance, focusing in the geochemical and mechanical evolution of all components and particularly on the bentonite plug and cementitious grout. The constitutive mechanical models include host rock creep, grout plasticity, steel degradation due to corrosion, and bentonite swelling upon hydration. Moreover, bentonite mechanical performance is coupled with reactive transport based on: montmorillonite (Mt) cation exchanger composition, porewater salinity, and Mt dissolution.

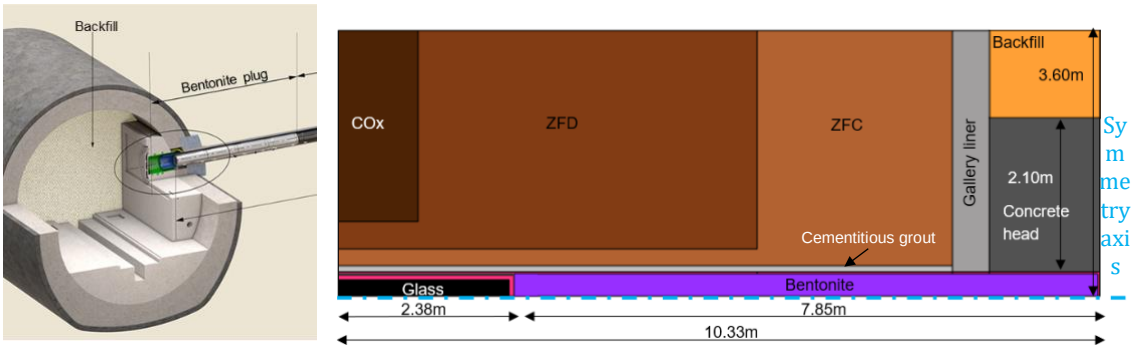

Figure 1: 3D concept for HLW disposal (from Andra) and 2D axisymmetric geometry of the cell system.

Use of COMSOL Multiphysics

Multiphase flow is simulated using Phase Transport in Porous Media and Darcy's Law coupled with Multiphase Flow in Porous Media interface. Solute transport is computed using Transport of Diluted Species in Porous Media interface. COMSOL Multiphysics has been coupled with PhreeqC (iCP) [1] to solve chemical reactions. Thereafter, the mechanical model is solved using Solid Mechanics interface with an external material library to solve a tailor-made BBMx implementation (seal) [2,3]. Extra Domain ODEs interfaces are used to solve steel corrosion and

host rock creep. Heat transfer is not explicitly solved but the spatio-temporal evolution of temperature is imported into COMSOL Multiphysics from a larger thermal analysis model.

Results

After repository closure, the system tends to resaturate with host rock porewater, but early gas generation from steel corrosion (preliminary calculations) leads to desaturation and late resaturation. Limited alkalinity, high diffusivity, and large contact area with the rock progressively lead to pH neutralization of the grout. Cement-bentonite interaction is significant near junctions between liner segments favouring the ingress of grout alkalinity (local alteration). From the mechanical point of view, host rock creep favours drift convergence throughout the simulation period. Initially, cell structures move slightly towards the rock due to H_2 gas generation by steel corrosion in the HLW cell, then converge due to creep. Injection of a highly-deformable grout has a significant impact in system evolution, partially absorbing radial displacements (both due to rock creep and gas pressure). Grout plasticity results in larger strains than stresses (no effect of creep transmitted to the bentonite seal) and bentonite plug and steel liner are less deformed (Figure 2).

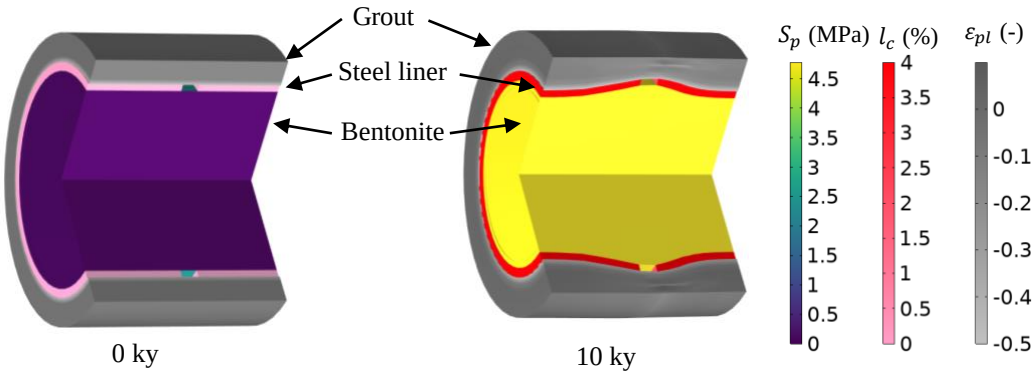

Figure 2: Bentonite swelling pressure (S_p), fraction of corroded steel liner (l_c), and volumetric plastic strain (ε_{pl}) in grout after 10 ky.

Conclusion

A 2D-axisymmetric THCM model of the HLW cell system has been successfully implemented. Temperature increase induced by waste packages, hydrogen generation from steel corrosion, geochemical interactions and dedicated constitutive models for each material are considered. Liner stiffness decays drastically due to corrosion while the grout absorbs drift convergence due to host rock creep. Therefore, bentonite-based seal loses strict confinement conditions, swelling radially and deforming the liner. As future work, the numerical representation of certain material interfaces/ interaction processes should be revisited or developed further, such as the couplings between hydraulic chemo-mechanical processes.

References

1. Nardi, A., Trinchero, P., de Vries, L. M., Molinero, J., Interface COMSOL-PHREEQC (iCP), an efficient numerical framework for the solution of coupled Multiphysics and geomchemistry. *Computers & Geosciences*, **69**, 10-21 (2014).
2. Laviña, M., Pelegrí, J., Idiart, A., Pasteau, A., Michau, N., Talandier, J., Cochepin, B., Long-term Evolution of Bentonite-Based Seals for Closure of a Radioactive Waste Repository in Claystone: A Hydro-Chemo-Mechanical Modelling Assessment, *Transport in Porous Media*, **151**, 287-317 (2024).
3. Pelegrí, J., Laviña, M., Bernachy-Barbe, F., Imbert, C., Idiart, A., Gaboreau, S., Cochepin, B., Michau, N., Talandier, J., Experimental and modelling study of the interaction of bentonite with alkaline water, *Applied Clay Science*, **245**, 107157 (2023)

Iberian COMSOL Multiphysics CONFERENCE
Málaga. June 28, 2024

P13

Optimal Resistive Load for Maximizing the Power Output of a Piezoelectric Harvester

Claudia Săvescu*[1,2], Daniel Comeagă[2], Mihaela Roman[1,2], Adrian Săvescu[1]

[1]Departament of Automation and Electrical Engineering, Romanian Research and Development Institute for Gas Turbines COMOTI
[2]Department of Mechatronics and Precision Mechanics, National University of Science and Technology Politehnica Bucharest
*Corresponding author: claudia.borzea@comoti.ro

Introduction

The paper studies the optimal load required for maximizing the power output of a quadmorph piezoelectric cantilever, comprising four PZT-5H layers [1]. An optimal load can maximize the power from piezoelectric harvesters [2].

Use of COMSOL Multiphysics

The quadmorph piezoelectric harvester geometry makes use of a 4 g tip constraining inertial mass, blocking the curvature on xOy plane that limits the electric output. The simulations employ a Multiphysics full coupling of Solid Mechanics and Electrostatics, via Piezoelectric Effect, using the strain-charge constitutive relations (Figure 1).

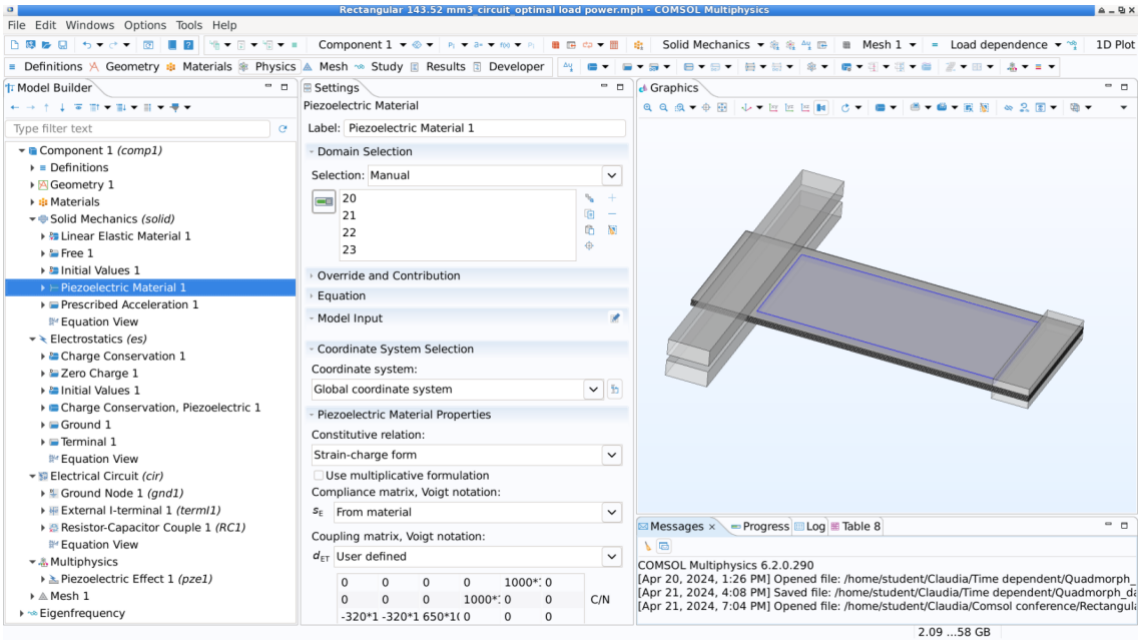

Figure 1: Simulation model.

The piezoelectric response is assessed by interconnecting:

- ***Solid Mechanics*:** declaring PZT-5H layers piezoelectric. An acceleration of 1 g is applied at the base of the bottom clamping bar. Mechanical damping is introduced as isotropic loss factor on the piezoelectric material.

- ***Electrostatics*:** Piezoelectric charge conservation is set for piezoelectric layers. Terminals type Circuit and ground are declared on the faces of the piezoelectric layers.
- ***Electrical circuit*:** The node connections are declared: 0 – ground, and 1 – External I-terminal, applying terminal voltage (es/term1) from Electrostatics to the circuit node. A resistor-capacitor couple declared in parallel.

Results

A frequency domain study, with 1 MΩ + 50 pF simulating spectrum analyser's impedance revealed the mechanical resonance at 171.2 Hz. The feeble maximum power, with a dominantly resistive load (cutoff frequency 3.183 kHz), was subsequently optimised within a load dependence frequency domain study, with an auxiliary sweep of the load resistor, *R_load*. We systematically narrowed the initial range of 0 ÷ 10 MΩ and refined the step around the maximum power point (Table 1).

The maximum power resulted with a 21 kΩ resistor, at 170.3 Hz (Figure 2). The resistor's dissipative nature causes the maximum power to occur at slightly lower frequency than the mechanical resonance.

Since we used a Resistor-Capacitor Couple (*RC1*), the power expression [3] considers the current through and voltage across resistor (*RC1_rcr*), as: 0.5*realdot(cir.RC1_rcr_i,cir.RC1_rcr_v).

Table 1: Simulation results

Frequency domain study	**Resistor *R_load***	**Capacitor**	**f_r [Hz]**	**f_{P_max} [Hz]**	**abs(*cir.RC1_rcr_v*) [V]**	**P_{max} @f_{P_max} [mW]**
Frequency domain, range(170,0.1,172) Hz	1 MΩ	50 pF	171.2	170.4	39.927	0.797
Load dependence, range(170.2,0.1,171.2) Hz, auxiliary sweep, *R_load*, range(10,1,50) kΩ	Optimal: 21 kΩ	50 pF	171.2	170.3	20.466	9.973

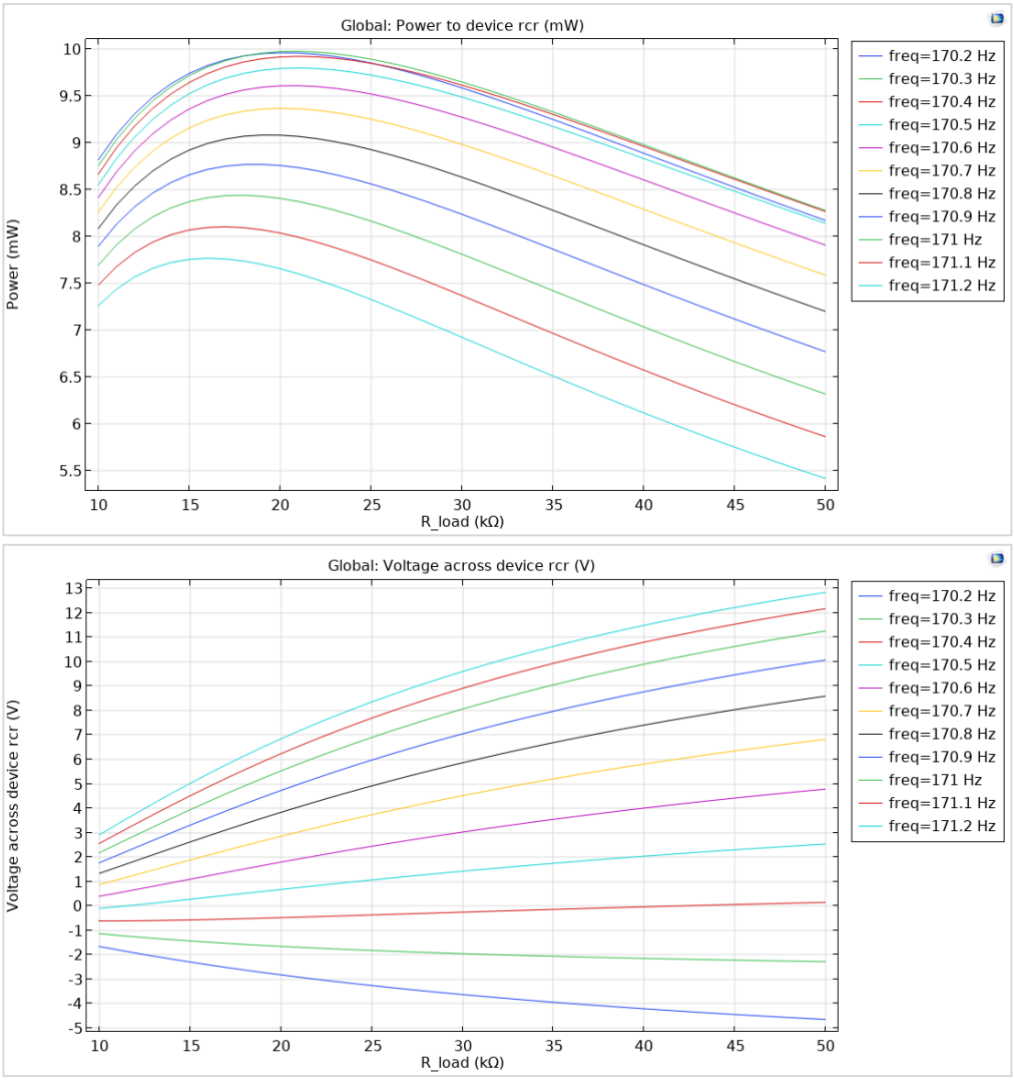

Figure 2: Power and voltage delivered to resistor.

Conclusion

This brief paper shows that an optimal load can boost the piezoelectric power output with more than one order of magnitude. We shall extend it into a full article, addressing the differences between the digital twin, testing in ideal laboratory conditions, and industrial conditions with circuitry components required for powering an energy harvesting circuit.

Acknowledgement

This paper was realised through “Nucleu” Program within Romanian Research, Development and Innovation Plan 2022-2027, conducted with the support of the Romanian Ministry of Research, Innovation and Digitalization, project number PN 23.12.01.02.

References

1. C. Borzea, C. Comeagă, and A. Săvescu, 'Boosting the Electric Output of a Cantilever Piezoelectric Harvester by Tip Curvature Blocking Elements', in ECRES 2020, Istanbul, Turkey, 2020, pp. 344–350.
2. O. Mokhiamar, D. O. Masara, and H. El Gamal, 'Performance Enhancement of Multi-Modal Piezoelectric Energy Harvesting Through Parameter Optimization', Jordan Journal of Mechanical and Industrial Engineering, **16**(5), pp. 677–688, 2022.
3. 'COMSOL Multiphysics Reference Manual. Version: COMSOL 6.2'. https://doc.comsol.com/6.2/doc/com.comsol.help.comsol/COMSOL_ReferenceManual.pdf.

Iberian COMSOL Multiphysics CONFERENCE
Málaga. June 28, 2024

P14

Thermoelectric Generator Simulations with and without Heatsink

Mihaela Roman[1,2], Claudia Săvescu*[1,2], Adrian Săvescu[1], Remus Stoica[1,2], Daniel Comeagă[2]

[1]Departament of Automation and Electrical Engineering, Romanian Research and Development Institute for Gas Turbines COMOTI
[2]Department of Mechatronics and Precision Mechanics, National University of Science and Technology Politehnica Bucharest
*Corresponding author: claudia.borzea@comoti.ro

Introduction

Thermoelectric generators (TEG) rely on the Seebeck effect. Their efficiency depends on the temperature difference between their hot side and cold side. Therefore, a heatsink is crucial to provide proper heat dissipation and cooling of the cold side. The paper herein shows how a heatsink boosts the power output of a TEG even in external natural convection with air. The temperature ranges considered were measured in-house on a screw compressor.

Use of COMSOL Multiphysics

The simulation model (Figure 1) relies on a real acquired 40 × 40 × 5 [mm] thermoelectric generator [1] with 72 n-p thermocouples of bismuth telluride, Bi_2Te_3. The simulations employ a full coupling of Heat Transfer in Solids and Electric Currents, via Thermoelectric Effect Multiphysics interface [2], for a complete modelling of Peltier-Seebeck-Thomson thermoelectric effects. Electromagnetic Heating is also coupled to account for resistive heating (Joule effect) [3].

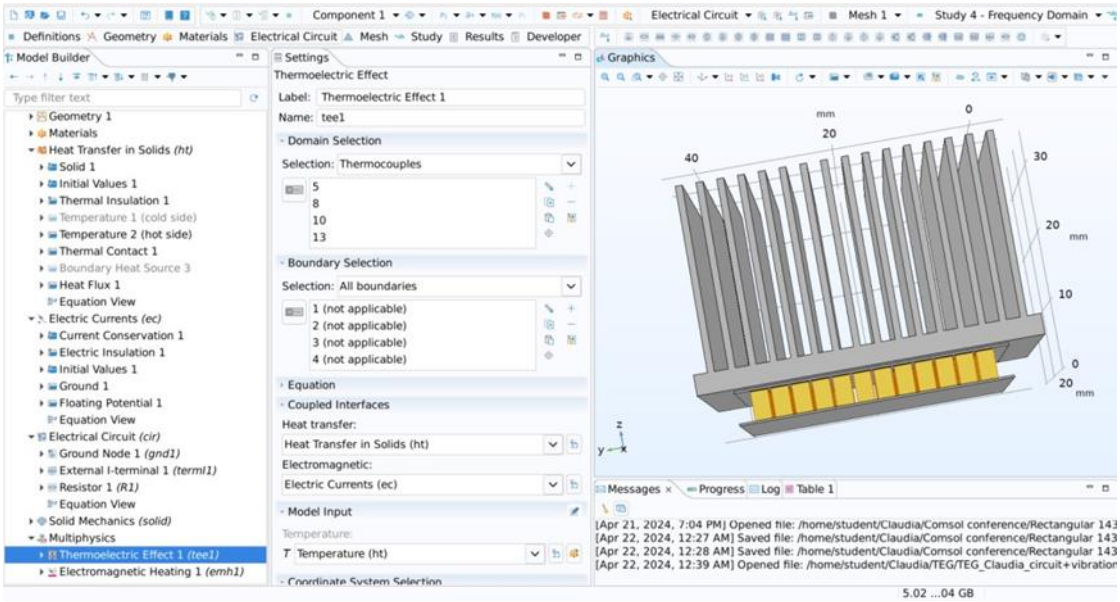

Figure 1: Simulation model with heatsink

The thermoelectric behaviour is assessed by interconnecting three physics:

- ***Heat Transfer in Solids*:** setting an initial hot side temperature, *Thot*, 100 degC, and declaringconvective heat flux (air natural convection at 1 atm, external temperature 20

degC). For the model with heatsink, thermal contact is set on TEG's cold side boundary.

- ***Electric Currents*:** Ground and a Floating Potential type Circuit are declared on the faces of the terminal legs (see [3]).
- ***Electrical circuit*:** The node connections are declared: 0 – ground, and 1 – External I-terminal,set to apply the floating potential (ec/fp1) from Electric Currents, relative to ground. A resistorof 2.4 kΩ (simulating a demo energy harvesting circuit) is declared in parallel.
- A stationary study with parametric sweep of *Thot*, range(30,5,100) degC, was conducted. A timedependent study, range(0,1,60) min, was also ran to see the thermal stabilization between hot andcold sides, with *Thot* = 100 degC.

Results

The graphs in Figure 2 show that the Stationary study is reliable to provide the results after thermal stabilization of the thermoelectric module, between the hot and cold sides. Additionally, the Time Dependent study offers extra information about the heatsink's effect on the electrical parameters, these ones decreasing more smoothly and maintaining values with almost one order of magnitude higher than without heatsink.

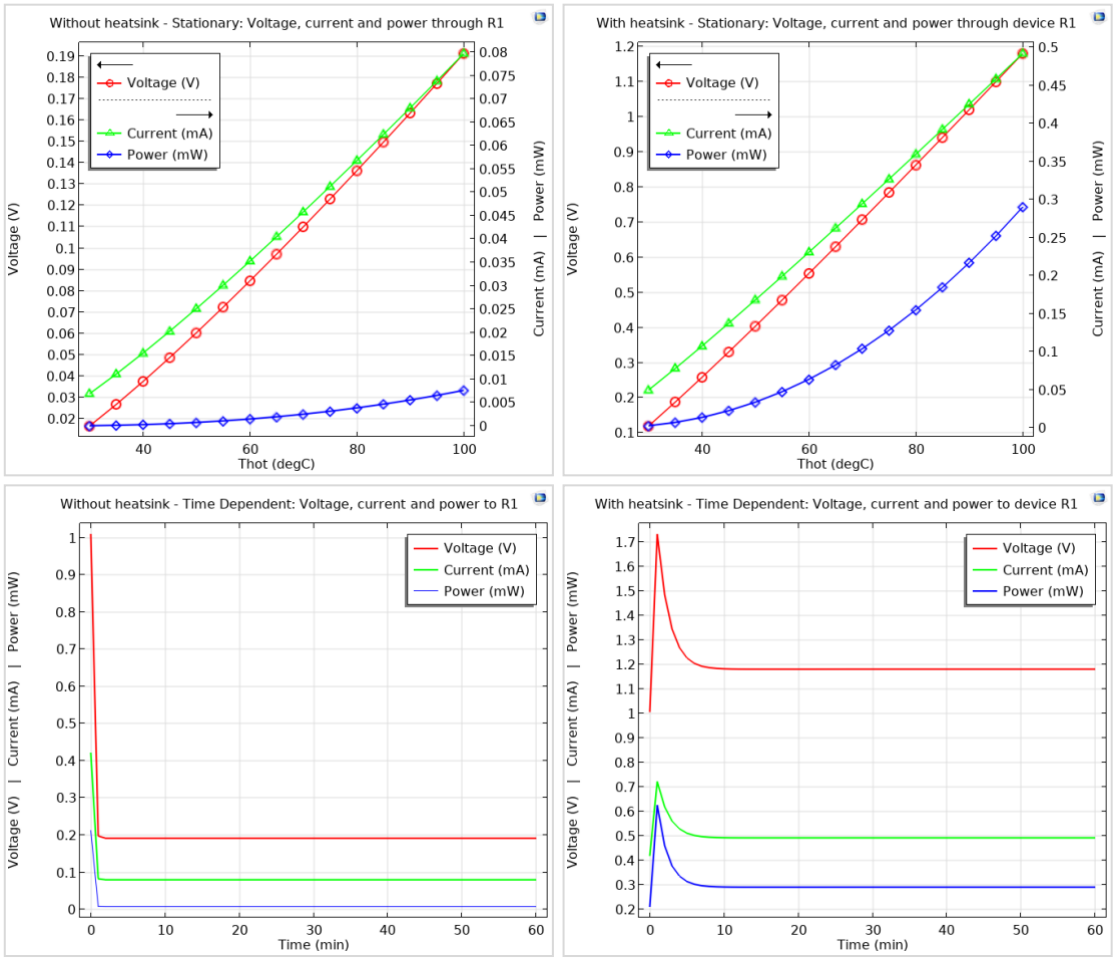

Figure 2: Voltage, current and power delivered to resistor

The computed power [4] considers the current and voltage through resistor (*R1*), written as: 0.5*realdot(cir.R1_i,cir.R1_v).

Conclusion

This brief paper herein shows that a heatsink improves the thermoelectric power output even in natural convection conditions. The numerical research will be extended into a full article, addressing the improvements in thermoelectric output with external forced convection. As well, the time dependent study shall be conducted with an auxiliary sweep of *Thot*.

Acknowledgement

This paper was realised through "Nucleu" Program within Romanian Research, Development and Innovation Plan 2022-2027, conducted with the support of the Romanian Ministry of Research, Innovation and Digitalization, project number PN 23.12.01.01.

References

1. TEGpro, 'TE-MOD-10W4V-40', www.tegpro.com. https://www.tegmart.com/datasheets/TGPR-10W4V-40S.pdf.
2. 'Thermoelectric Cooler', COMSOL. https://www.comsol.com/model/thermoelectric-cooler-30611.
3. C. Săvescu, A. Morega, Y. Veli, and V. Petrescu, 'Numerical Modelling of Thermoelectric Energy Harvesting from Industrial Compressor Waste Heat', in *2023 13th International Symposium on Advanced Topics in Electrical Engineering (ATEE)*, 2023, pp. 1–6. doi: 10.1109/ATEE58038.2023.10108390.
4. 'COMSOL Multiphysics Reference Manual. Version: COMSOL 6.2.' https://doc.comsol.com/6.2/doc/com.comsol.help.comsol/COMSOL_ReferenceManual.pdf.

Committees

Scientific Committee

- Ed Fontes. *COMSOL AB, Stockholm, Sweden.*
- Eduardo González Tapia. *COMSOL AB, Stockholm, Sweden.*
- Emilio Ruiz Reina. *University of Málaga, Spain.*
- Ricardo Torres Cámara. *Polytechnic University of Catalonia, Spain*.
- Juan Manuel Paz García. *University of Málaga, Spain.*
- Benjamín Ivorra. *Complutense University of Madrid, Spain.*
- Rubén Picó Vila. *University of Valencia, Spain.*
- José Manuel González Vida. *University of Málaga, Spain.*

Organizing Committee

Emilio Ruiz Reina
Department of Applied Physics II, University of Malaga.
eruizr@uma.es

Araceli Sánchez-Guitard López-Valera
Department of Applied Physics II, University of Malaga.
seliara@hotmail.com

Juan Antonio Rubio Sancho D'Ávila
Addlink Scientific Software, S.L.
jrubio@addlink.es

Antonio Molina Castellano
Addlink Scientific Software, S.L.
amolina@addlink.es

Carlos David González Gómez
Department of Applied Physics II, University of Malaga
cdgg@uma.es